

A novel series solution to the renormalization group equation in QCD

B A Magradze

A. Razmadze Mathematical Institute, M. Aleksidze St. 1, Tbilisi 0193, Georgia

E-mail: magr@rmi.acnet.ge

Abstract.

Recently, the QCD renormalization group (RG) equation at higher orders in MS-like renormalization schemes has been solved for the running coupling as a series expansion in powers of the exact 2-loop order coupling. In this work, we prove that the power series converges to all orders in perturbation theory. Solving the RG equation at higher orders, we determine the running coupling as an implicit function of the 2-loop order running coupling. Then we analyze the singularity structure of the higher order coupling in the complex 2-loop coupling plane. This enables us to calculate the radii of convergence of the series solutions at the 3- and 4-loop orders as a function of the number of quark flavours n_f . In parallel, we discuss in some detail the singularity structure of the $\overline{\text{MS}}$ coupling at the 3- and 4-loops in the complex momentum squared plane for $0 \leq n_f \leq 16$. The correspondence between the singularity structure of the running coupling in the complex momentum squared plane and the convergence radius of the series solution is established. For sufficiently large n_f values, we find that the series converges for all values of the momentum squared variable $Q^2 = -q^2 > 0$. For lower values of n_f , in the $\overline{\text{MS}}$ scheme, we determine the minimal value of the momentum squared Q_{min}^2 above which the series converges. We study properties of the non-power series corresponding to the presented power series solution in the QCD Analytic Perturbation Theory approach of Shirkov and Solovtsov. The Euclidean and Minkowskian versions of the non-power series are found to be uniformly convergent over whole ranges of the corresponding momentum squared variables.

PACS numbers: 11.10.Hi, 12.38.Aw, 12.38.Bx, 02.30.Mv

1. Introduction

It is known that the QCD running coupling at the 2-loop order in MS-like (massless) renormalization schemes can be solved explicitly as a function of the scale in terms of the Lambert W function [1, 2, 3]. The Lambert W function is the multivalued solution of

$$W_k(z) \exp\{W_k(z)\} = z, \quad (1)$$

the branches of W are denoted $W_k(z)$, $k = 0, \pm 1, \dots$. An exhaustive review of the Lambert- W function may be found in ref. [4]. The relevant branch of $W(z)$ which is

used to determine the coupling depends on the number of light quark flavours n_f . For a real positive momentum squared Q^2 † (and above the Landau singularity if $0 \leq n_f \leq 8$) the 2-loop coupling takes the form

$$\alpha_s^{(2)}(Q^2, n_f) = \begin{cases} -(\beta_0/\beta_1)(1 + W_{-1}(z_Q))^{-1}, & \text{if } 0 \leq n_f \leq 8 \\ -(\beta_0/\beta_1)(1 + W_0(z_Q))^{-1}, & \text{if } 9 \leq n_f \leq 16 \end{cases} \quad (2)$$

where $z_Q = -(eb_1)^{-1}(Q^2/\Lambda^2)^{-1/b_1}$, β_0 and β_1 are the first two β -function coefficients, $b_1 = \beta_1/\beta_0^2$ and $\Lambda \equiv \Lambda_{\overline{\text{MS}}}$ is the conventional $\overline{\text{MS}}$ scheme QCD parameter. Using formula (2), the analytical structure of the 2-loop coupling in the complex Q^2 plane was determined [1, 2, 5]. The motivation for these studies was a need for the development of dispersive methods [6-25]. The dispersive approach has been devised to extend properly modified perturbation theory calculations towards the low-energy region [6, 7, 15]. The most simple and elaborated variant of the dispersive approach, the Shirkov-Solovtsov Analytic Perturbation Theory (APT), was formulated in refs. [7] and [9] (for a review on APT and many original references see refs. [10] and [24]). It should be remarked that in the time-like region APT is equivalent to the ‘‘contour improved perturbation theory’’ proposed previously in ref. [26] (see also refs. [27-31]). The relation between this framework and APT was discussed in refs. [12, 32]. More sophisticated nonperturbative modifications of the (minimal) analytic QCD model of Shirkov and Solovtsov were also presented [18-23]. A generalization of APT to non-integer (fractional) powers of the running coupling has also been proposed and successfully used to calculate the three-point functions in QCD [23].

The 2-loop explicit solution (2) was soon found to have a more important application. In ref. [33], the running coupling in the k -th order ($k \geq 3$) in a MS-like renormalization scheme was expanded in powers of the exact two-loop order coupling (here and hereof we omit the argument n_f)

$$\alpha_s^{(k)}(Q^2) = \sum_{n=1}^{\infty} c_n^{(k)} \alpha_s^{(2)n}(Q^2). \quad (3)$$

On this basis, author of ref. [33] has proposed a new method for reducing the scheme ambiguity for QCD observables. A similar expansion (motivated differently for an observable depending on a single scale) was suggested in ref. [34]. Note that the analogical expansion but in powers of the approximate (asymptotic) 2-loop coupling has previously been introduced in ref. [35]. This expansion was used to construct the running coupling with consistent matching conditions at the quark thresholds in the 3-loop order. However, if the asymptotic 2-loop coupling is used, the coefficients of the expansion depend on the scale Q^2 . The main advantage of (3) is that it allows us to write QCD observables, in massless renormalization schemes, as series in powers of the renormalization scheme independent quantity, the exact explicit 2-loop coupling (2). One could introduce a similar expansion in powers of the 1-loop scheme independent coupling as well. However such a series would not be useful, since it could not describe

† Here $Q^2 = -q^2 = -(q^0)^2 + \vec{q}^2$ and $Q^2 > 0$ in the Euclidean domain.

the double logarithmic singularities of the higher order coupling. Recently, the series (3) has been used to construct exact explicit expressions for Euclidean and Minkowskian observables within APT [32, 36] (see also ref. [31]). In practice, the first few terms in series (3) give the excellent approximations to the coupling even in the infrared region [32, 36]

The main purpose of this paper is to present a detailed mathematical investigation of the series (3). In Sect. 2 we discuss in some details the singularity structure of the $\overline{\text{MS}}$ coupling, in higher orders, in the complex Q^2 plane. In particular, we determine the locations of the Landau singularities of the coupling (at the 3- and 4-loops) as a function of n_f for the n_f values into the range of validity of the asymptotic freedom of QCD. A similar investigation (but for large n_f values when the β -function has a positive fixed point) has previously been undertaken by the authors of refs. [16, 17] using a different technique, whose work does not overlap the material in Sect. 2 to a marked extent. In Sect. 3 we prove that the series (3) in the MS-like renormalization schemes has a positive radius of convergence to all orders in perturbation theory. In the proof we use the methods of the analytical theory of differential equations. In Sect. 4 we solve a higher-order RG equation for the running coupling implicitly as a function of the 2-loop running coupling. By means of the obtained transcendental equation, we determine the analytical structure of the higher order coupling in the complex 2-loop coupling plane. As a result, we evaluate analytically the radii of convergence of series (3) at 3- and 4-loops as a function of n_f . In Sect. 5 we determine the convergence region of the series solution with respect to the momentum squared variable Q^2 . For sufficiently large n_f values ($n_f \geq 14$ in the $\overline{\text{MS}}$ scheme), we find that the series converges for all $Q^2 > 0$. For the lower n_f values, we determine the minimal value Q_{min}^2 above which the series converges. We compare this scale, at $n_f = 3$, with the infrared boundary of perturbative QCD estimated within two different nonperturbative frameworks. In Sect. 6 we study properties of the dispersive images of the series solution (3), the non-power series determined in the sense of the QCD Analytic Perturbation Theory approach of Shirkov and Solovtsov, both in the space- and time-like regions. Our conclusions are given in Sect. 7. In the Appendix we collect some relevant formulas which we need in our computations.

2. The Analytic Structure of the Coupling to Higher Orders

In this section, we will determine the location of the Landau singularities of the coupling in the complex Q^2 plane at the 3-loop and 4-loop orders. As we shall see, there is a close relation between these singularities and the convergence properties of the series (3). For large n_f values ‡, we will reproduce part of the results of [16, 17] using another technique. Let us first give some familiar aspects of the RG equation in the way we prefer

‡ Note that QCD as a realistic theory appears only for 6 flavours and below. However, there are different theoretical motivations to consider the multi-flavour theory for $6 < n_f \leq 16$ (see, for example, [37, 38, 39]).

to formulate it. It is more convenient to introduce the dimensionless variable $u = Q^2/\Lambda^2$ and a modified running coupling, $a(u) = \beta_0\alpha_s(Q^2)$, satisfying the RG equation

$$u \frac{da(u)}{du} = \bar{\beta}^{(k)}(a(u)) = - \sum_{n=0}^{k-1} b_n a^{n+2}(u) \quad (4)$$

where $\bar{\beta}^{(k)}(a) = \beta_0\beta^{(k)}(a/\beta_0)$ and $b_n = \beta_n/\beta_0^{n+1}$ (for our notations see the Appendix). The \overline{MS} scheme values of the first three coefficients $b_{1,2,3}$ are listed in Table A.1. With this normalization of the coupling relevant perturbative formulas in higher order applications of renormalization group become simple [8, 19, 27]. Suppose that the solution to (4) $a(u)$ has a singularity at some finite point, $u = u_L$, in the complex u -plane, i.e. $a(u) \rightarrow \infty$ as $u \rightarrow u_L$. It follows then from the differential equation (4) that

$$a^{(k)}(u) \approx (u_L^{(k)}/(u - u_L^{(k)}))^{1/k} \quad \text{as } u \rightarrow u_L^{(k)}.$$

However, to confirm the existence of the singularities and to determine their positions, a detailed investigation is required in each finite order of perturbation theory.

Let us integrate Eq. (4) for sufficiently large real positive values of $u = \exp(t)$ in the neighborhood of a real point $u_0 = \exp(t_0)$

$$t = \ln u = T^{(k)}(a) \quad \text{where} \quad T^{(k)}(a) = \int_{a_0}^a \{\bar{\beta}^{(k)}(a')\}^{-1} da' + t_0, \quad (5)$$

this can also be written

$$t = a^{-1} + b_1 \ln(a) + \tilde{T}^{(k)}(a) + \tilde{t}_0, \quad (6)$$

where $\tilde{T}^{(k)}(a)$ is a regular at zero function

$$\tilde{T}^{(k)}(a) = \int_{a_0}^a G^{(k)}(a') da' : \quad G^{(k)}(a) = 1/\bar{\beta}^{(k)}(a) + 1/a^2 - b_1/a, \quad (7)$$

here the integration constant has been redefined: $\tilde{t}_0 = t_0 - a_0^{-1} - b_1 \ln(a_0)$. The conventional definition of the scale Λ parameter [40] leads us to the condition $\tilde{t}_0 = -\tilde{T}^{(k)}(0)$ §. With this choice Eq. (6) reads

$$t = a^{-1} + b_1 \ln(a) + \int_0^a G^{(k)}(a') da'. \quad (8)$$

We could write in place of (8) another but related formula [41]

$$t = a^{-1} - b_1 \ln(b_1 + a^{-1}) + \int_0^a g^{(k)}(a') da' \quad (9)$$

where

$$g^{(k)}(a) = (\bar{\beta}^{(k)}(a))^{-1} - (\bar{\beta}^{(2)}(a))^{-1} = (1 + b_1 a)^{-1} \left(\sum_{n=0}^{k-1} b_n a^n \right)^{-1} \sum_{n=2}^{k-1} b_n a^{n-2}, \quad (10)$$

and $\bar{\beta}^{(2)}(a)$ is the 2-loop $\bar{\beta}$ -function. The function $T^{(k)}(a)$ can be expressed in terms of the elementary functions. In the 3-loop case, we can write

$$T^{(3)}(a) = a^{-1} + b_1 \ln(a) + T_1^{(3)}(a) - T_1^{(3)}(0), \quad (11)$$

§ the term proportional to $1/\ln^2(u)$ in the asymptotic expansion of $a(u)$ at large u should be suppressed.

where

$$T_1^{(3)}(a) = \begin{cases} -0.5b_1 \ln(P^{(3)}(a)) + \frac{2b_2 - b_1^2}{\sqrt{\Delta^{(3)}}} \arctan\left(\frac{b_1 + 2b_2a}{\sqrt{\Delta^{(3)}}}\right) & \text{if } 0 \leq n_f \leq 5 \\ \frac{\ln(a - a_1)}{(a_1 - a_2)(1 + b_1a_1)} - \frac{\ln(a_2 - a)}{(a_1 - a_2)(1 + b_1a_2)} & \text{if } 6 \leq n_f \leq 16, \end{cases} \quad (12)$$

$P^{(3)}(a) = b_2a^2 + b_1a + 1$, $\Delta^{(3)} = 4b_2 - b_1^2$, and $a_{1,2} = (-b_1 \pm \sqrt{-\Delta^{(3)}})/(2b_2)$. In the $\overline{\text{MS}}$ scheme $\Delta^{(3)} > 0$ (< 0) if $0 \leq n_f \leq 5$ ($6 \leq n_f \leq 16$) (see Tables 1 and 2).

Let us specify the locations of the roots of the algebraic equation

$$P^{(k)}(a) = \bar{\beta}^{(k)}(a)/a^2 = -\sum_{n=0}^{k-1} b_n a^n = 0, \quad (13)$$

the non-trivial zeros of the $\bar{\beta}$ function, for different values of n_f . For $0 \leq n_f \leq 7$, in the 4-loop order in the $\overline{\text{MS}}$ scheme equation (13) has one negative real root $a_1 < 0$ and a pair of complex conjugate roots $a_2 = \bar{a}_3$ (see Table 3). We will assume that $\Im(a_2) < 0$. Then Eq. (8) can be written as

$$t = a^{-1} + b_1 \ln(a) + T_1^{(4)}(a) - T_1^{(4)}(0), \quad (14)$$

where $T_1^{(4)}(a)$ is a regular at zero function

$$T_1^{(4)}(a) = -b_3^{-1} \left\{ E_1 \ln(a - a_1) + \Re(E_2) \ln[(a - a_2)(a - a_3)] + 2\Im(E_2) \arctan\left(\frac{a - \Re(a_2)}{|\Im(a_2)|}\right) \right\}, \quad (15)$$

with

$$E_i = \{a_i^2(a_i - a_j)(a_i - a_k)\}^{-1}, \quad i \neq j \neq k$$

and (i, j, k) is a cyclic permutation of $(1, 2, 3)$. Equation (15) was derived for real positive values of a . It may be continued analytically in the complex a -plane choosing the relevant branches for each elementary function on the right hand side. For unphysical values $8 \leq n_f \leq 16$, in the 4-loop case Eq. (13) has three real roots: $a_1 < 0$, $0 < a_2 < a_3$ (see Table 4). Let a be positive lying in the interval $0 < a < a_2$. Formula (8) may now be rewritten

$$t = a^{-1} + b_1 \ln(a) - b_3^{-1} \sum_{i=1}^3 E_i \ln(a_i^{-1}(a_i - a)). \quad (16)$$

For complex values of a , the analytical continuation of Eq. (16) can be easily performed assuming that each logarithm on the right of (16) have its principal value.

We have to determine the analytical continuation of the coupling starting from the implicit solution (5). This implies a preliminary study of the analytical properties of the inverse function $t = T^{(k)}(a)$ in the complex coupling plane. The one-valued branch of this function may be defined in the cut complex a -plane choosing the cuts carefully. The physical branch may be determined from the requirement that the branch yields a real positive t for real positive and sufficiently small values of a . It is convenient to determine the analytical continuation of $T^{(k)}(a)$ starting directly from the integral representation

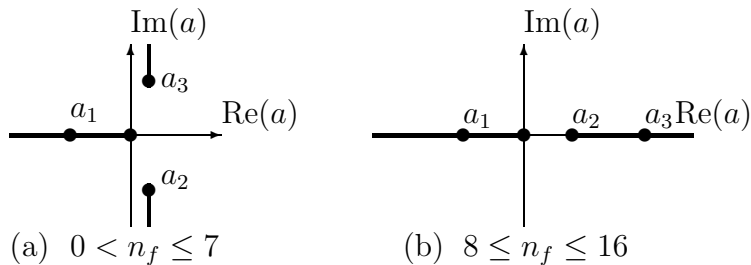


Figure 1. The singularity structure of the function $t = T^{(4)}(a)$. Two different situations are shown. Branch cuts are represented by bold lines and branch points by the blobs.

(9). The integral there should be regarded as a line integral in the complex a -plane. The line must be deformed to avoid singularities of the integrand. It is seen from (6) that the function $T^{(k)}(a)$ has a simple pole as well as a logarithmic branch point at $a = 0$. In addition, there are logarithmic singularities at the roots of the algebraic equation (13). For $0 < n_f \leq 5$, in the 3-loop case (in the $\overline{\text{MS}}$ scheme) Eq. (13) has a pair of complex conjugate roots, while it has two real (positive and negative) roots for $6 \leq n_f \leq 16$ (see Tables 1 and 2). The 4-loop case has already been discussed above. We must make a branch cut along the negative a -axis $\{a : -\infty < a < 0\}$ corresponding to the logarithmic branch point at zero. In the cases, where there is a pair of complex conjugate branch points (say $a_{2,3}$ in the 4-loop case) we must choose additional branch cuts. One possibility is to choose the cuts parallel to the imaginary axis (see Fig. 1(a)), so that these branch points are connected by the cut running through the infinity. In the 4-loop case, we choose the cuts $\{a : -\infty < \Im(a) < \Im(a_2), \Im(a_3) < \Im(a) < \infty, \Re(a) = \Re(a_3)\}$ (see Fig. 1(a)). The analytical continuation of $T^{(k)}(a)$ in the cut complex a -plane will be determined uniquely if we require that $T^{(k)}(a)$ is real for a real positive and sufficiently small values of a . Note that the above considered choice for the cuts is not unique. We could, for example, choose the cuts running along straight lines connecting the complex conjugate branch points to the origin. Nevertheless, former possibility (which we accept in this paper) seems to be preferable: with this choice t as a function of the phase of a will be continuous in the neighborhood of $a = 0$ with the exception of the cut running along the negative a -axis.

Consider now the theoretical cases with only real roots. Let a_1 be the negative root, and a_2 be the positive one (in the 4-loop case a_2 is the smallest positive root). Then the branch cuts may be chosen along the real intervals $\{a : -\infty < a < 0\}$ and $\{a : a_2 < a < \infty\}$ (see Fig. 1(b)). To determine the physical branch, we require that $T^{(k)}(a)$ is real in the real interval $a \in (0, a_2)$. We may now analyze the singularity structure of the running coupling $a = \tilde{a}(t) \equiv a(u)$ in the complex t -plane, and hence in

the complex u -plane too. Evidently, the singular points are determined by the limiting values of the function $T^{(k)}(a)$ as a tends to infinity \parallel . In general, the limiting values may depend on the way along which a tends to infinity. Consider, for example, the 3-loop case for $6 \leq n_f \leq 16$. We start from formula (11). Let a be a point in the complex plane $a = |a| \exp(i\delta)$, where δ is the phase of a . The analytical continuation to this point gives

$$T^{(3)}(a) = \exp(-i\delta)|a|^{-1} - 0.5b_1 \ln(|P^{(3)}(a)||a|^{-2}) - \frac{0.5b_1^2 - b_2}{\sqrt{-\Delta^{(3)}}} \ln \left| \frac{a_2(a - a_1)}{-a_1(a_2 - a)} \right| + i(b_1\delta - 0.5b_1(\delta_1 + \delta_2) - (0.5b_1^2 - b_2)(\delta_1 - \delta_2)/\sqrt{-\Delta^{(3)}}), \quad (17)$$

where $P^{(3)}(a) = b_2a^2 + b_1a + 1$ ($b_2 < 0$) and δ_i ($i = 1, 2$) denote the increments of the arguments of $(\tilde{a} - a_1)$ and $(a_2 - \tilde{a})$ as \tilde{a} goes from 0 to the point a along a contour Γ : $\delta_1 = \Delta_\Gamma \arg(\tilde{a} - a_1)$ and $\delta_2 = \Delta_\Gamma \arg(a_2 - \tilde{a})$. We can now calculate limiting values of $T^{(3)}(a)$ as a tends to the sides of the branch cuts along the real axis. We find, at the sides,

$$\begin{aligned} \delta = 0, \quad \delta_1 = 0, \quad \delta_2 = \mp\pi, & \quad \text{if } \operatorname{Re}(a) > a_2, \operatorname{Im}(a) = \pm\epsilon \\ \delta = \pm\pi, \quad \delta_1 = \pm\pi, \quad \delta_2 = 0, & \quad \text{if } \operatorname{Re}(a) < a_1, \operatorname{Im}(a) = \pm\epsilon \end{aligned} \quad (18)$$

where $\epsilon \rightarrow 0^+$ is assumed. Using Eq. (17) with Eq. (18), we may easily calculate the limits of $T^{(3)}(a)$ when a goes to infinity along the upper or lower side of the right (left) cut. One may confirm that the result will be the same regardless of the branch cut chosen. It depends only on the side of the cut: $t_\pm^{(3)}(n_f) = \lim_{a \rightarrow \infty} T^{(3)}(a \pm i\epsilon) = \lim_{a \rightarrow -\infty} T^{(3)}(a \pm i\epsilon)$. Thus we find, for $6 \leq n_f \leq 16$,

$$t_\pm^{(3)}(n_f) = -0.5b_1 \ln |b_2| + \frac{b_2 - 0.5b_1^2}{\sqrt{-\Delta^{(3)}}} \ln |a_2/a_1| \pm i \left(0.5b_1 + \frac{b_2 - 0.5b_1^2}{\sqrt{-\Delta^{(3)}}} \right) \pi. \quad (19)$$

Consider now the 4-loop case for $8 \leq n_f \leq 16$. Using arguments similar those employed in the 3-loop case, we find the singular points

$$t_\pm^{(4)}(n_f) = b_3^{-1} \sum_{k=1}^3 E_k \ln |a_k| \pm i(E_2 + E_3)\pi. \quad (20)$$

Now it is sufficient to show that the obtained limits do not depend on the special choice of the directions in the complex a -plane. To see this, let us take the contour integral in Eq. (9) along a closed contour chosen as follows. Let the contour consists of two different curves with common starting point at zero. Let both curves lie in the upper (lower) complex plane and are connected by the arc of a circle with centre at zero and radius R . The integrand has no singularity inside the contour, and the value of the integral is therefore zero (the Cauchy's theorem). Consider the limit when the radius of the circle tends to infinity. Then the integral along the arc tends to 0. So that the integrals along the two different curves tend to the same limit. Thus the result stated follows.

It is important to determine whether or not the singular points $t_\pm^{(k)}(n_f)$ are located inside the strip $-\pi < \Im(t) \leq \pi$. The strip is image of the first (physical) sheet of the

\parallel we assume that the coupling does not have singular points where it takes finite values.

complex Q^2 plane under $t = \ln(Q^2/\Lambda^2)$. Depending on the value of n_f there are two cases to consider. The first case is that the points lie inside the strip so that the unphysical Landau singularities appear in the first sheet. Then the running coupling is not causal, and thus perturbation theory is incomplete: the non-perturbative contributions are required to remove the unphysical singularities [1, 7, 15, 16]. This case corresponds to real-world QCD, where $n_f \leq 6$. In the second case, the singular points may arise beyond the strip. So that there are not real or complex singularities on the first sheet of the momentum squared variable, and thus perturbation theory is consistent with causality. The singularities still may present only on the time-like axis $Q^2 < 0$. The second possibility may be realized for sufficiently large n_f values. The value of n_f above which the causal analytical structure of the coupling is restored can be found from the equation

$$\Im\{t^{(k)}(n_f^*)\} = \pm\pi. \quad (21)$$

With the 3-loop formula (19), we find the solution to (21) $n_f^{*(3)} \approx 8.460$, and with the 4-loop formula (20) $n_f^{*(4)} \approx 8.455$. Thus, the 3- and 4-loop $\overline{\text{MS}}$ scheme results almost coincide. We remark that the 3-loop estimation was obtained previously in [16]. The 2-loop condition for causality of the coupling can be found in [1]. In our notation it reads $b_1(n_f) \leq -1$, this gives for the lower boundary of the causal region the value $n_f^{*(2)} \approx 9.68$.

Note that for $n_f > n_f^*$ the β -function has a positive infrared stable fixed point (see Tables 2 and 4). So that the running coupling is trapped in the range between 0 (the ultraviolet fixed point) and the infrared fixed point at all energies. The fact that QCD in perturbation theory for sufficiently large n_f values has an infrared fixed point has long been discussed [37]. Of particular interest is the case when the fixed value of the coupling is sufficiently small. Then, presumably, the theory may be reliably described within perturbation theory for all energies including infrared region. The corresponding interval of n_f values is called as a conformal window [3, 16, 17, 38]. It is believed that there is a phase transition in QCD with respect to n_f inside the range of validity of asymptotic freedom $0 \leq n_f \leq 16$. For small values of n_f below the critical point ($n_f < N_f^{\text{cr}} < 16$) the theory is defined via the confining phase. Above this point, there is a conformal window $N_f^{\text{cr}} < n_f \leq 16$, where the theory is defined via the non-Abelian Coulomb phase with no color confinement and dynamical chiral symmetry breaking. One possible way to determine the critical point is to use the Oehme-Zimmermann criterion for the gluon confinement, the superconvergence rule for the transverse gluon propagator [39]. This gives the value $N_f^{\text{cr}} = 13N_c/4$ ($=9.75$ for $N_c = 3$ colours). Other possibility is to apply arguments of dynamical chiral symmetry breaking [3, 38, 42, 43]. This gives slightly large value $N_f^{\text{cr}} \approx 4N_c$. Assuming the value for N_f^{cr} as predicted by the superconvergence rule, the authors of [16, 17] have given arguments that the perturbative running coupling inside the conformal window (and beyond the 1-loop approximation) is always causal, i.e. $n_f^* < N_f^{\text{cr}}$. Note that the infrared fixed value of the coupling inside the window is not large: it coincides with the root a_2 (in the 3-loop

case, for $n_f = 10$, $a_2 \approx 0.26$).

Consider now the cases where Eq. (13) has complex roots. In the $\overline{\text{MS}}$ scheme this takes place at 3-loops if $0 \leq n_f \leq 5$ and at 4-loops if $0 \leq n_f \leq 7$. The corresponding cuts in the a -plane are chosen as shown in Fig. 1(a). We first calculate the limit of $T^{(k)}(a)$ as a tends to infinity along a line going to infinity in the right half-plane $\Re(a) > \Re(a_2)$. Evidently, the result will not depend on the particular choice of the direction as far as the line belongs to the right-half plane $\Re(a) > \Re(a_2)$. Choosing the path along the positive semi-axis and using the 3- and 4-loop formulas (12) and (15), we calculate the limits, $t_{\text{rhp}}^{(k)}(n_f) = \lim_{a \rightarrow \infty} T^{(k)}(a)$,

$$t_{\text{rhp}}^{(3)}(n_f) = -0.5b_1 \ln(b_2) + \frac{2b_2 - b_1^2}{\sqrt{\Delta^{(3)}}} \left(\frac{\pi}{2} - \arctan \left(\frac{b_1}{\sqrt{\Delta^{(3)}}} \right) \right), \quad (22)$$

$$\begin{aligned} t_{\text{rhp}}^{(4)}(n_f) &= b_3^{-1} \left(-2\Im(E_2) \left(0.5\pi + \arctan \left[\frac{\Re(a_2)}{|\Im(a_2)|} \right] \right) \right. \\ &\quad \left. + E_1 \ln |a_1| + 2\Re(E_2) \ln |a_2| \right), \end{aligned} \quad (23)$$

here the subscript ‘‘rhp’’ shows that the limits are calculated along the way going to infinity through the right half plane $\Re(a) > \Re(a_2)$. Let us now calculate the limits of $T^{(k)}(a)$ when a tends to infinity through the left half plane $\Re(a) < \Re(a_2)$. We may take without loss of generality the ways along the sides of the cut running on the negative semi-axis. The limiting values of $T^{(k)}(a)$ from above and below the cut, $T_{\pm}^{(k)}(a) = \lim_{\epsilon \rightarrow 0^+} T^{(k)}(a \pm i\epsilon)$, may be determined by the analytical continuation of the right hand sides of Eqs. (11) and (14). The singularities are then determined by the limiting values $t_{\text{lh}\pm}^{(k)} = \lim_{a \rightarrow -\infty} T_{\pm}^{(k)}(a)$. This gives

$$t_{\text{lh}\pm}^{(3)}(n_f) = t_{\text{rhp}}^{(3)}(n_f) - \pi(2b_2 - b_1^2)/\sqrt{\Delta^{(3)}} \pm i\pi b_1, \quad (24)$$

$$t_{\text{lh}\pm}^{(4)}(n_f) = t_{\text{rhp}}^{(4)}(n_f) + 2\pi\Im(E_2)/b_3 \pm i\pi(b_1 - E_1/b_3). \quad (25)$$

Equivalently, by the analytical continuation of (9) for negative values of a we obtain the useful formula

$$t_{\text{lh}\pm}^{(k)}(n_f) = -b_1 \ln b_1 + p.v. \int_0^{-\infty} g^{(k)}(a') da' \pm i\pi(b_1 + \text{res}[g^{(k)}(a), a_1^{(k)}]), \quad (26)$$

where $a_1^{(k)}$ denote the real negative root of (13) (which presents only in the 4-th order case) and the integral here is considered in the ‘‘principal value sense’’ (p.v.). It is seen from the Tables 1 and 3 that in these cases the Landau singularities present in the first sheet of the Q^2 -plane.

3. The Proof of the Convergence of the Series

Inserting series (3) into the RG equation (A.1), we recursively determine the coefficients $\{c_n^{(k)}\}_{n=3}^{\infty}$ in terms of c_2 ($c_1 = 1$) and the β -function coefficients. However, the coefficient $c_2^{(k)}$ still remains undetermined. This reflects the arbitrariness in the definition of the Λ -parameter. With the conventional definition of the parameter, we find that $c_2^{(k)} = 0$.

Table 1. The 3-loop $\overline{\text{MS}}$ quantities: the complex zeros of the $\bar{\beta}$ -function $a_{1,2}$, and the singularity locations $t_{\text{rhp}}^{(3)}$ and $t_{\text{lh}\pm}^{(3)}$ in the t -plane as a function of n_f for $0 \leq n_f \leq 5$.

n_f	$a_{1,2}$	$t_{\text{rhp}}^{(3)}$	$t_{\text{lh}\pm}^{(3)}$
0	$-0.393 \pm 0.882i$	0.844	$-1.539 \pm 2.648i$
1	$-0.399 \pm 0.892i$	0.839	$-1.506 \pm 2.628i$
2	$-0.415 \pm 0.916i$	0.830	$-1.433 \pm 2.578i$
3	$-0.447 \pm 0.965i$	0.810	$-1.293 \pm 2.482i$
4	$-0.526 \pm 1.071i$	0.766	$-1.026 \pm 2.322i$
5	$-0.819 \pm 1.349i$	0.650	$-0.423 \pm 2.067i$

Table 2. Same as in Table 2, but for $6 \leq n_f \leq 16$.

n_f	a_1	a_2	$t_{\pm}^{(3)}$
6	-1.49	7.09	$0.173 \mp 0.077i$
7	-0.877	1.24	$-0.159 \mp 1.05i$
8	-0.651	0.660	$-0.019 \mp 2.36i$
9	-0.509	0.409	$0.620 \mp 4.26i$
10	-0.403	0.264	$2.17 \mp 7.21i$
12	-0.245	0.104	$13.6 \mp 21.3i$
14	-0.125	0.028	$98.7 \mp 89.9i$
16	-0.023	0.001	$6216 \mp 2852i$

Table 3. The 4-loop $\overline{\text{MS}}$ quantities for $0 \leq n_f \leq 7$.

n_f	a_1	$a_{2,3}$	$t_{\text{rhp}}^{(4)}$	$t_{\text{lh}\pm}^{(4)}$
0	-0.797	$0.130 \mp 0.782i$	1.164	$-1.294 \pm 0.961i$
1	-0.794	$0.134 \mp 0.784i$	1.163	$-1.284 \pm 0.930i$
2	-0.793	$0.142 \mp 0.792i$	1.158	$-1.256 \pm 0.871i$
3	-0.796	$0.159 \mp 0.810i$	1.145	$-1.199 \pm 0.768i$
4	-0.802	$0.190 \mp 0.844i$	1.114	$-1.099 \pm 0.593i$
5	-0.806	$0.259 \mp 0.906i$	1.035	$-0.940 \pm 0.295i$
6	-0.795	$0.444 \mp 1.012i$	0.821	$-0.707 \mp 0.217i$
7	-0.741	$1.124 \mp 0.973i$	-0.047	$-0.423 \mp 1.074i$

Table 4. Same as in Table 4, but for $8 \leq n_f \leq 16$.

n_f	a_1	a_2	a_3	$t_{\pm}^{(4)}$
8	-0.623	0.699	6.476	$-0.093 \mp 2.37i$
9	-0.482	0.426	4.810	$0.522 \mp 4.28i$
10	-0.362	0.281	1.937	$1.95 \mp 7.32i$
12	-0.193	0.112	0.548	$13.1 \mp 21.9i$
14	-0.085	0.030	0.196	$98.1 \mp 91.8i$
16	-0.014	0.001	0.031	$6219 \mp 2858i$

This follows from Eqs. (2) and (3) if we use the asymptotic expansion for the Lambert- W function (see pp. 22-23 in [4])

$$W_k(z) = L_1 - L_2 + L_2/L_1 + L_2(-2 + L_2)/2L_1^2 + L_2(6 - 9L_2 + 2L_2^2)/6L_1^3 + O((L_2/L_1)^4) \quad (27)$$

where for the branch $W_{-1}(z)$ for real negative z ($z \rightarrow 0^-$ as $Q^2 \rightarrow \infty$) we must put $L_1 = \ln(-z)$ and $L_2 = \ln(-\ln(-z))$. Several first coefficients calculated in the 4-loop case are: $c_1^{(4)} = 1$, $c_2^{(4)} = 0$, $c_3^{(4)} = \beta_2/\beta_0$, $c_4^{(4)} = \beta_3/2\beta_0$,

$$c_5^{(4)} = \frac{5}{3} \frac{\beta_2^2}{\beta_0^2} - \frac{\beta_1\beta_3}{6\beta_0^2}, \quad c_6^{(4)} = -\frac{1}{12} \frac{\beta_1\beta_2^2}{\beta_0^3} + \frac{1}{12} \frac{\beta_3\beta_1^2}{\beta_0^3} + 2 \frac{\beta_2\beta_3}{\beta_0^2}, \dots$$

Inserting these values of the coefficients into series (3) and using (27), one may readily reproduce the conventional asymptotic representation for the coupling (see, for example, [44])

$$\alpha_{\text{asy}}(Q^2) = \frac{1}{\beta_0 L} - \frac{\beta_1 \ln L}{\beta_0^3 L^2} + \frac{1}{\beta_0^3 L^3} \left(\frac{\beta_1^2}{\beta_0^2} (\ln^2 L - \ln L - 1) + \frac{\beta_2}{\beta_0} \right) + O\left(\frac{\ln^3 L}{L^4}\right), \quad (28)$$

where $L = \ln(Q^2/\Lambda^2) \gg 1$.

Let us change the variable according to $Q^2 \rightarrow \theta = \beta_0 \alpha_s^{(2)}(Q^2)$ and introduce the new function $w(\theta) \equiv w^{(k)}(\theta) = \alpha_s^{(k)}(Q^2)/\alpha_s^{(2)}(Q^2) - 1$. The RG equation (A.1) may be rewritten as

$$\theta \frac{dw}{d\theta} = f^{(k)}(\theta, w), \quad (29)$$

where

$$f^{(k)}(\theta, w) = \frac{(w+1)^2}{1+b_1\theta} \sum_{n=0}^{k-1} b_n \theta^n (1+w)^n - (w+1), \quad (30)$$

with $b_n = \beta_n/\beta_0^{n+1}$. The function of two variables $f^{(k)}(w, \theta)$ has the Taylor expansion

$$f^{(k)}(w, \theta) = \sum_{m,n=0}^{\infty} \eta_{m,n}^{(k)} w^m \theta^n, \quad (31)$$

with $\eta_{0,0}^{(k)} = 0$, $\eta_{1,0}^{(k)} = 1$ and $\eta_{0,1}^{(k)} = 0$. In the 4-loop case, the expansion is

$$f^{(4)}(w, \theta) = w + b_1 \theta w + b_2 \theta^2 + w^2 + (b_3 - b_1 b_2) \theta^3 + \dots \quad (32)$$

We may now use the analytical theory of differential equations [45, 46] to investigate Eq. (29). With the initial condition $w(0) = 0$, this equation has a singularity: for $\theta = 0$ and $w = 0$ the ratio $f^{(k)}(\theta, w)/\theta$ is undefined. Nevertheless, in the special case where $\eta_{0,0}^{(k)} = 0$, $\eta_{1,0}^{(k)} = 1$ and $\eta_{0,1}^{(k)} = 0$, Eq. (29) may still have an analytic solution satisfying the initial condition $w(0) = 0$ (see e.g. [45] and [46]). For the sake of clarity, the following discussion is quite detailed. The expansion (31) converges in the domain $D = \{0 < |w| < r_1, 0 < |\theta| < r_2\}$, where r_1 and r_2 are some positive numbers chosen in the range $\{r_1, r_2 : r_1 < \infty, r_2 < 1/|b_1|\}$. It follows then from the classical theory that there exists a positive number $M^{(k)}$ such that $|f^{(k)}(w, \theta)| \leq M^{(k)}$ for $(w, \theta) \subset D$, and the coefficients $\eta_{m,n}^{(k)}$ satisfy the inequalities [45, 46]

$$|\eta_{m,n}^{(k)}| \leq \xi_{m,n}^{(k)}, \quad \text{where} \quad \xi_{m,n}^{(k)} = M^{(k)} r_1^{-m} r_2^{-n}. \quad (33)$$

Under these conditions, we will show that there exists a regular solution to Eq. (29)

$$w(\theta) \equiv w^{(k)}(\theta) = \sum_{n=2}^{\infty} \bar{c}_n^{(k)} \theta^n, \quad (34)$$

where $\bar{c}_n^{(k)} = \beta_0^{-n} c_{n+1}^{(k)}$, with $c_n^{(k)}$ being the coefficients in the original series (3). We recall that according to our choice $\bar{c}_1^{(k)} = \beta_0^{-1} c_2^{(k)} = 0$. Inserting expansions (31) and (34) into Eq. (29) we recursively determine the coefficients $\bar{c}_n^{(k)}$

$$\bar{c}_2^{(k)} = \eta_{0,2}^{(k)}, \quad 2\bar{c}_3^{(k)} = \eta_{1,1}^{(k)} \bar{c}_2^{(k)} + \eta_{0,3}^{(k)}, \dots \quad (35)$$

Consider now the auxiliary function $\tilde{w} = \tilde{w}(\theta)$ satisfying the equation

$$\tilde{w} = f_1^{(k)}(\tilde{w}, \theta) \equiv \frac{M^{(k)}}{(1 - \tilde{w}/r_1)(1 - \theta/r_2)} - M^{(k)} \left(1 + \frac{\tilde{w}}{r_1} + \frac{\theta}{r_2} \right), \quad (36)$$

it has the Taylor expansion

$$f_1^{(k)}(\tilde{w}, \theta) = \sum_{m=0, n=0} \xi_{m,n}^{(k)} \tilde{w}^m \theta^n, \quad (37)$$

with the coefficients $\xi_{m,n}^{(k)}$ defined in (33). Equation (36) has a series solution

$$\tilde{w}(\theta) \equiv \tilde{w}^{(k)}(\theta) = \sum_{n=2}^{\infty} \gamma_n^{(k)} \theta^n. \quad (38)$$

Inserting the expansions (37) and (38) into Eq. (36) we find the recurrence formulas

$$\gamma_2^{(k)} = \xi_{0,2}^{(k)}, \quad \gamma_3^{(k)} = \xi_{1,1}^{(k)} \gamma_2^{(k)} + \xi_{0,3}^{(k)}, \dots \quad (39)$$

Let us compare Eqs. (35) with Eqs. (39). Making use of Eq. (33), we obtain the inequalities $|\bar{c}_n^{(k)}| < \gamma_n^{(k)}$ for $n = 2, 3, \dots$. It follows then from the comparison test that the series (34) is absolutely convergent in the disk of convergence of the series (38). Evidently, the series (38) has a positive radius of convergence. The radius is equal to the modulus of the nearest to the origin singularity $\theta_{\text{nr}}^{(k)}$ of the function $\tilde{w} = \tilde{w}(\theta)$. The value \tilde{w} can be solved explicitly from the quadratic equation (36). The singularities of the majorant function $\tilde{w}(\theta)$ are therefore located at the zeros of the discriminant of the quadratic equation. Hence we find the singular points

$$\theta_1^{(k)} = r_2, \quad \theta_2^{(k)} = -r_1 r_2 / M^{(k)}, \quad \theta_{3,4}^{(k)} = r_2 (-l^{(k)} / 2 - 1 \pm \sqrt{l^{(k)2} + 8l}), \quad (40)$$

where $l^{(k)} = 1 + r_1 / M^{(k)}$. To obtain the best possible estimation, we have to maximize $|\theta_{\text{nr}}^{(k)}|$ with respect to r_1 and r_2 . The quantity $M^{(k)} = \max_{w, \theta} |f^{(k)}(w, \theta)|$ may be determined according to the maximum modulus principle. The modulus $|f^{(k)}(w, \theta)|$ takes its maximum on the circles $|w| = r_1$ and $|\theta| = r_2$. We find that the maximum of $|f^{(k)}(w, \theta)|$ is attained for real positive values of w and θ . Furthermore, $\theta_{\text{nr}}^{(k)} = \theta_3^{(k)}$. We choose the values $r_1 = 0.25$ and $r_2 = 0.42$ in the 3-loop case, while $r_1 = 0.21$ and $r_2 = 0.32$ in the 4-loop case. Using ‘‘Maple 7’’ [47], we determine numerically the maximal values of $|f^{(k)}(w, \theta)|$ on these circles. For $n_f = 3$, we have found that $M^{(3)} \approx 0.695$ and $M^{(4)} \approx 0.596$. Computing the modulus of the numbers (40) and comparing them, we determine the radii of convergence of the majorant series (38):

$\tilde{\rho}_{maj}^{(3)} = |\theta_3^{(3)}| \approx 0.045$ and $\tilde{\rho}_{maj}^{(4)} = |\theta_3^{(4)}| \approx 0.033$. Thus we have found that the radii of convergence of the original series (3) in the $\overline{\text{MS}}$ scheme in the 3- and 4-loop orders, at $n_f = 3$, are bounded below as $\rho^{(3)} \geq \tilde{\rho}_{maj}^{(3)}/\beta_0 \approx 0.06$ and $\rho^{(4)} \geq \tilde{\rho}_{maj}^{(4)}/\beta_0 \approx 0.05$. As we shall see, the actual values of $\rho^{(k)}$ are significantly larger than the obtained lower bounds.

We remark that the above proof of the convergence of the series holds in all MS-like (massless) renormalization schemes, since in the proof we have not used specific values of the β -function coefficients and the condition $c_2 = 0$ is common for all these schemes.

4. Determination of the Radius of Convergence of the Series

By a change of variable $Q^2 \rightarrow \theta = a^{(2)}(u)$ ($u = Q^2/\Lambda^2$) Eq. (4) can be rewritten

$$\frac{da}{d\theta} = \frac{\sum_{n=0}^{k-1} b_n a^{n+2}}{\theta^2 + b_1 \theta^3}, \quad (41)$$

where $a = F^{(k)}(\theta) = a^{(k)}(u) \equiv \beta_0 \alpha_s^{(k)}(Q^2)$. In the following we will sometimes, but not always, omit the superscript “ (k) ” referring to the order of perturbation theory. In the preceding section, we have shown that the series (34) or equivalently the series

$$a = F(\theta) = \sum_{n=1}^{\infty} \tilde{c}_n \theta^n, \quad (\tilde{c}_n = \beta_0^{-n+1} c_n) \quad (42)$$

has a positive convergence radius. It is possible then to define the inverse function $\theta = F^{-1}(a)$, which can be expanded in powers of a

$$\theta = F^{-1}(a) = \sum_{n=1}^{\infty} d_n a^n. \quad (43)$$

By using arguments similar to those employed in Sect. 3, one can verify that the series (43) also has a finite radius of convergence. Under this condition, we may apply the classical method for estimating the convergence radius of series (see the book [48] pp. 146-148). The main argument is that the function $a = F(\theta)$ must have at least one singular point on the circle of convergence of the series (42). There are two possible cases. First, suppose that θ_0 be a finite singularity of $F(\theta)$, where the function takes a finite value, $a_0 = F(\theta_0) < \infty$, while its derivative does not exist. In terms of the inverse function $\theta = F^{-1}(a)$ these conditions read

$$\left. \frac{dF^{-1}(a)}{da} \right|_{a=a_0} = 0. \quad (44)$$

Using Eq. (41) at $\theta = \theta_0$, we may rewrite Eq. (44) in the form

$$\left. \frac{d\theta}{da} \right|_{a=a_0} = \frac{\theta_0^2(1 + b_1 \theta_0)}{\sum_0^{k-1} b_n a_0^{n+2}} = 0, \quad (45)$$

for a finite a_0 (which is not a root of $\sum_0^{k-1} b_n a_0^n = 0$) Eq. (45) has only two solutions: $\theta_0 = 0$ and

$$\theta_0 = -1/b_1 \quad (= -81/64 \quad \text{for} \quad n_f = 3). \quad (46)$$

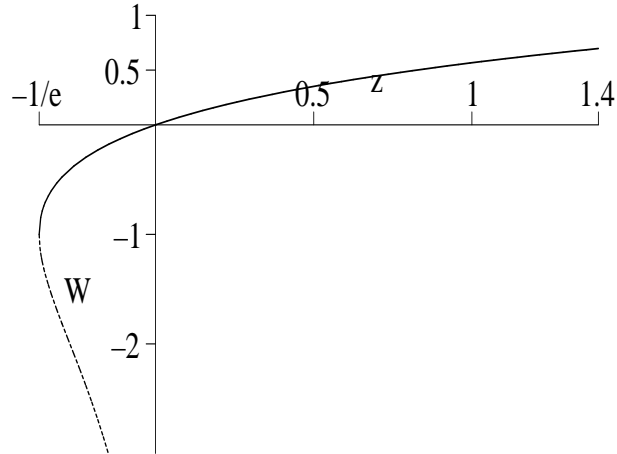


Figure 2. The two real branches of $W(z)$. The solid line corresponds to $W_0(z)$ and the dotted line in the range $W < -1$ refers to $W_{-1}(z)$.

The solution $\theta_0 = 0$ must be rejected, since at $\theta = 0$ Eq. (45) does not hold because of the initial condition $F(\theta)/\theta \rightarrow 1$ as $\theta \rightarrow 0$ (see (42)). Secondly, suppose that there exists a curve C going to infinity in the domain of analyticity of $\theta = F^{-1}(a)$ such that $F^{-1}(a) \rightarrow \theta_s < \infty$ as a tends to infinity along this curve. Then, $F(\theta)$ has a singularity at $\theta = \theta_s$.

First, we shall consider Eq. (41) in the 3- and 4-loop orders for $0 \leq n_f \leq 5$ and $0 \leq n_f \leq 7$ respectively. Let us integrate Eq. (41) in the real range $\{\theta, a : \theta > 0, a > 0\}$. We write the result in the symmetrical form

$$1/\theta - b_1 \ln(b_1 + 1/\theta) = 1/a - b_1 \ln(b_1 + 1/a) + \int_0^a g^{(k)}(a') da', \quad (47)$$

where the function $g^{(k)}(a)$ is defined by (10), and we have determined the integration constant according to the previous choice (see Sect. 2). Equation (47) may be continued for complex values of a and θ . Then the integral with respect to a should be regarded as a line integral in the complex a -plane. The contour connecting the origin to a must avoid singular points of the integrand.

Note that all the coefficients in series (42) are real, so are the coefficients in the inverse series (43). Therefore, θ as a function of a must be real for real values of a provided that a is any point inside the circle of convergence of the inverse series. It is seen from Eq. (41) that there exists a real neighborhood of the origin $\theta = 0$, where the function $F(\theta)$ is real and strictly increasing. Thus, in the 3-loop case, the derivative $F'(\theta) > 0$ if $\theta > -1/b_1$, provided that $0 \leq n_f \leq 5$ ($b_1 > 0$). In the 4-loop case, the same is true if $\theta > \max(-1/b_1, a_1^{(4)})$, where $a_1^{(4)}$ is the real negative root of the equation (13), ($a_1^{(4)}(n_f = 3) \approx -0.796$). From this with the initial condition $F^{-1}(0) = 0$, it follows that there exists a sufficiently small real interval including the origin, where the function $\theta = F^{-1}(a)$ is real and strictly increasing. Inside this interval $F^{-1}(a) > 0$ ($F^{-1}(a) < 0$) if $a > 0$ ($a < 0$). Fortunately, we may solve the transcendental equation (47) for θ

explicitly as a function of a in terms of the Lambert-W function

$$\theta = F^{-1}(a) = -b_1^{-1}(1 + W_n(z))^{-1}, \quad (48)$$

where $z = \zeta(a) = -(eb_1)^{-1} \exp(-T(a)/b_1)$, and

$$T(a) = a^{-1} - b_1 \ln(b_1 + a^{-1}) + \int_0^a g(a') da'. \quad (49)$$

It follows from the above discussion that in the region $a > 0$ inside the convergence disc of the series (43) (where $\theta > 0$) the required branch in Eq. (48) is $W_{-1}(z)$, so that

$$\theta = F^{-1(k)}(a) = -b_1^{-1}(1 + W_{-1}(\zeta^{(k)}(a)))^{-1}. \quad (50)$$

Formula (50) may be continued beyond the convergence circle on the positive a -semi-axis. It follows from (49) that the function $z = \zeta(a)$ is negative and monotonically decreasing in the infinite interval $a \in (0, \infty)$. For the considered values of n_f (with the exception of $n_f = 7$ case at 4-loops) $\zeta(a)$ takes values in the range $(-e^{-1}, 0^-)$ for $a \in (0, \infty)$. The branch $W_{-1}(z)$ is real and negative with $W_{-1}(z) \in (-\infty, -1)$ for $z \in (-e^{-1}, 0^-)$ (see Fig. 2). Therefore, the function $\theta = F^{-1}(a)$ determined by (50) is real and positive in the entire positive a -semi-axis. However, in the 4-loop case at $n_f = 7$, we find that $z \in (-e^{-1}, 0^-)$ only inside the interval $a \in (0, a_b)$ where $a_b \approx 1.003$, and $z < -e^{-1}$ if $a > a_b$. Since $W_{-1}(z)$ has a branch point at $z = -e^{-1}$, the function $F^{-1(4)}(a)$ at $n_f = 7$ will have a branch point at $a = a_b$. The corresponding branch cut may be chosen along the positive interval $\{a : a_b < a < \infty\}$. Formula (50) still holds on the upper side of the cut: on the sides of the cut the function $F^{-1(4)}(a)$ at $n_f = 7$ takes complex conjugate values. Using (50), we calculate the limit of $F^{-1}(a)$ as $a \rightarrow \infty$ along the positive a -semi-axis. So we find a singularity of the function $a = F(\theta)$

$$\theta_{s,1}^{(k)} = -b_1^{-1}(1 + W_{-1}(\zeta^{(k)}(\infty)))^{-1} = a^{(2)}(u_{\text{rhp}}^{(k)}), \quad (51)$$

here we have used the formula

$$\zeta^{(k)}(\infty) = \lim_{a \rightarrow +\infty} \zeta^{(k)}(a) = -(b_1 e)^{-1} \exp(-T^{(k)}(\infty)/b_1) = -(b_1 e)^{-1} (u_{\text{rhp}}^{(k)})^{-1/b_1}, \quad (52)$$

where $u_{\text{rhp}}^{(k)} = \exp(t_{\text{rhp}}^{(k)})$ being the Landau singularity located on the positive u -semi-axis (see the 3-and 4-loop formulas (22) and (23)). The last equality in (52) follows from Eq. (9). In the 4-loop order, at $n_f = 7$, we find a pair of complex conjugate singular points, $\theta_{s,1\pm} = \lim_{a \rightarrow +\infty} \Theta(a \pm i0)$, where $\theta_{s,1+}$ is determined by (51).

Formally we may continue Eq. (47) for negative real values of the variables in the region $\{a, \theta : -1/b_1 < a < 0, -1/b_1 < \theta < 0\}$. Assuming that each logarithm in Eq. (47) have its principal value, we obtain in this region the equation

$$1/\theta - b_1 \ln(1/|\theta| - b_1) = 1/a - b_1 \ln(1/|a| - b_1) + \int_0^a g(a') da'. \quad (53)$$

Note that the right-hand side of Eq. (53) is in fact regular at $a = -1/b_1$: the logarithmic singularities of the last two terms are cancelled in the sum. For negative values of a , the path of integration of the integral on the right of (53) goes along negative a -axis, but avoids the poles of $g(a)$ by small semi-circles above or below the axis. Equation (53)

Table 5. Locations of the extra singularities in the a -plane at the 3- and 4-loop orders.

n_f	$a_{b_{\pm}}^{(3)}$	$ a_{b_{\pm}}^{(3)} $	$a_{b_{\pm}}^{(4)}$	$ a_{b_{\pm}}^{(4)} $
0	$0.038 \pm 0.732i$	0.733	$0.156 \pm 0.600i$	0.616
1	$0.038 \pm 0.741i$	0.742	$0.159 \pm 0.600i$	0.620
2	$0.039 \pm 0.762i$	0.763	$0.166 \pm 0.609i$	0.632
3	$0.042 \pm 0.806i$	0.807	$0.179 \pm 0.629i$	0.654
4	$0.046 \pm 0.902i$	0.904	$0.207 \pm 0.668i$	0.700
5	$0.060 \pm 1.186i$	1.187	$0.275 \pm 0.744i$	0.793
6			$0.498 \pm 0.888i$	1.018
7			1.003	1.003

has exactly one real negative solution for θ inside the interval $a \in (\tilde{a}, 0)$, where $\tilde{a} = -\infty$ in the 3-loop order and it is the finite negative root of (13) in the 4-loop order. This solution is determined in terms of the branch $W_0(z)$

$$\theta = F^{-1(k)}(a) = -b_1^{-1}(1 + W_0(\tilde{\zeta}^{(k)}(a)))^{-1}, \quad (54)$$

where $\tilde{\zeta}^{(k)}(a) = (eb_1)^{-1} \exp(-\tilde{T}^{(k)}(a)/b_1)$ and

$$\tilde{T}^{(k)}(a) = a^{-1} - b_1 \ln(-a^{-1} - b_1) + \int_0^a g^{(k)}(a') da'. \quad (55)$$

It is instructive to check that our choice for the branches on the real a -axis in fact follows from the analytical continuation. To see this, let us expand expressions (50) and (54) as $a \rightarrow 0^+$ and $a \rightarrow 0^-$ respectively. We must use expansion (27) for $W_{-1}(z)$ as $z \rightarrow 0^-$. The same formula, but with $L_1 = \ln \tilde{z}$ and $L_2 = \ln \ln \tilde{z}$ holds for $W_0(\tilde{z})$ as $\tilde{z} \rightarrow \infty$ (see formula (4.19) in ref. [4]). One may verify that both expansions reproduce the same convergent power series (43). So that Eqs. (50) and (54) represent the same analytical function in two different regions. Let us now discuss the analytical structure of the function $\theta = F^{-1}(a)$ starting from Eq. (48). In general, $F^{-1}(a)$ may have singularities at the same points where $T(a)$ is singular. Nevertheless, as we have shown, $F^{-1}(a)$ is regular at $a = 0$, while $T(a)$ is singular there. Furthermore, $F^{-1}(a)$ may have additional singularities $a_{b_{\pm}}$ arising due to the common branch point of $W_0(z)$ and $W_{\pm 1}(z)$ at $z = -e^{-1}$. To determine locations of these singularities we numerically solve the equation

$$z = \zeta^{(k)}(a) = -e^{-1} \quad (56)$$

at the 3- and 4 loop orders. The approximate locations of these singularities for different n_f values are given in Table 5. Note that not all roots of Eq. (56) give rise to the singularities of $F^{-1}(a)$ on the first sheet of the Riemannian surface. Thus in the 4-loop case, for $n_f = 7$, Eq. (56) has the roots $a_{b_{\pm}} \approx 0.16 \pm 0.40i$. But one may verify that these points are not singular on the first sheet. To make the function $\theta = F^{-1}(a)$ single valued, we must draw cuts in the complex a -plane taking into account the branch points of $T(a)$ and those of W function. We draw cuts in the complex a -plane attached to the complex conjugate branch points (say $a_{2,3}$ in the 4-loop case, the roots of (13)) and running to infinity parallel to the imaginary a axis: $\{a : \Re(a) = \Re(a_{2,3}), -\infty <$

$\Im(a) < \Im(a_2)$, $\Im(a_3) < \Im(a) < \infty$ }. In the 4-loop case, we must draw an extra cut attached to the real branch point at $a_1 < 0$ and running along the negative semi-axis $\{a : -\infty < a < a_1\}$. We also make the branch cuts running parallel to the imaginary axis $\{a : \Re(a) = \Re(a_{b\pm}), -\infty < \Im(a) < \Im(a_{b-}), \Im(a_{b+}) < \Im(a) < \infty\}$ attached to the branch points at $a_{b\pm}$, the roots of Eq. (56). However, in the 4-loop case, for $n_f = 7$, the branch cut must be chosen along the positive real axis $\{a : 1.003 < a < \infty\}$. With this choice of the cuts, the function $\theta = F^{-1}(a)$ will be analytic in the disc with centre the origin and radius $r_c = \min\{|a_{b\pm}|, |a_i|\}$ ($a_i, i = 1, 2 \dots$ denote the roots of Eq. (13)). For $0 \leq n_f \leq 5$, the points $a_{b\pm}$ are closest to the origin singularities both in the 3- and 4-loop orders. Let us define $a = r \exp(i\delta)$ and $z = \zeta(a) = |z| \exp(i\Phi)$, where

$$|z| = (eb_1)^{-1} \exp(-\Re T(a)/b_1) \quad \text{and} \quad \Phi = \pi - \Im T(a)/b_1. \quad (57)$$

Let a describes the semi-circle of radius $r < r_c$ lying in the upper half plane ($0 \leq \delta \leq \pi$) starting from the positive semi-axis. Then the image under $z = \zeta(a)$ describes a curve in the z -plane. This curve intersects the real negative z -semi-axis for two or more times at different points. The number of the intersections depends on the value of r : it increases when r decreases. At the intersections the boundary of the branch of W is reached, so that the branch of W -function must be changed when z passes these points. To define the analytical continuation along the semi-circle, we demand that the function $\theta = F^{-1}(a) \equiv \tilde{F}^{-1}(\zeta(a))$ will be continuous as a function of the phase of a . This will be achieved, if we use the rules of counter-clockwise continuity [4] for selecting the branches of W when the curve crosses the branch cut. These rules are given by

$$\begin{aligned} W_{-1}(x + i0) &= W_1(x - i0) & \text{if} & \quad -e^{-1} < x < 0 \\ W_1(x - i0) &= W_0(x + i0) & \text{if} & \quad -\infty < x < -e^{-1} \\ W_n(x + i0) &= W_{n+1}(x - i0) & \text{if} & \quad -\infty < x < 0 \quad \text{and} \quad n \geq 1. \end{aligned} \quad (58)$$

We start at $a = r < r_c$ on the positive semi-axis with the branch $W_{-1}(z)$ and pass the semi-circle $\{\delta : 0 \leq \delta \leq \pi\}$ selecting the relevant branches according to the rules (58). Using ‘‘Maple 7’’ [47], we have plotted the function $z = \zeta(a)$ along the semi-circles for various values of r in the interval $0 < r < r_c$. In this way, we have determined the variations of the phase $\Phi = \arg(z)$ along the semi-circles. Then we have confirmed that the analytical continuation on the negative interval $-r_c < a < 0$, with the rules (58), really leads to the branch $W_0(z)$.

Having the analytical structure of $F^{-1}(a)$ established, we can construct explicit expressions for $F^{-1}(a)$ in the entire cut complex a -plane. This enables us to calculate the limits of $F^{-1}(a)$ as a tends to infinity along different directions in the complex plane and determine thereby the singularities of the function $a = F(\theta)$ in the complex θ -plane. Using the arguments based on Cauchy’s theorem (see Sect. 2), one may justify that it is sufficient to calculate the limits choosing the directions only along the real a -axis.

Let us now define the analytical continuation along entire negative a -semi-axis. In the 3-loop case, we may represent (55) in the form

$$\tilde{T}^{(3)}(a) = a^{-1} - b_1 \ln(|a|^{-1} - b_1) + \text{p.v.} \int_0^a g^{(3)}(a') da' \quad (59)$$

Table 6. Positions of the singularities in the θ -plane at the 3-loop order.

n_f	0	1	2	3	4	5
θ_0	-1.186	-1.195	-1.219	-1.266	-1.353	-1.520
$\theta_{s,1}^{(3)}$	0.627	0.635	0.653	0.691	0.776	1.029
$\theta_{s,2}^{(3)}$	-0.594	-0.601	-0.618	-0.653	-0.731	-0.956
$\tilde{\rho}$	0.594	0.601	0.618	0.653	0.731	0.956

for all $a < 0$. Thus $\tilde{T}^{(3)}(a)$ is real, and therefore $\tilde{\zeta}^{(3)}(a) > 0$ for all $a < 0$. Hence $W_0(\tilde{\zeta}^{(3)}(a)) > 0$ (see Fig. 2), so that $F^{-1(3)}(a) < 0$ for all $a < 0$. It is evident that the required branch, in this case, will be $W_0(z)$ on the entire negative a -semi-axis. Making $a \rightarrow -\infty$ in Eq. (54) and using Eq. (59), we find the real singular point

$$\theta_{s,2}^{(3)} = \lim_{a \rightarrow -\infty} F^{-1(3)}(a) = -(b_1(1 + W_0(\tilde{\zeta}^{(3)}(-\infty))))^{-1} \quad (60)$$

where $\tilde{\zeta}^{(3)}(-\infty) = (eb_1)^{-1} \exp(-\tilde{T}^{(3)}(-\infty)/b_1)$, and

$$\tilde{T}^{(3)}(-\infty) = \lim_{a \rightarrow -\infty} \tilde{T}^{(3)}(a) = -b_1 \ln b_1 - \text{p.v.} \int_{-\infty}^0 g^{(3)}(a) da = \Re(t_{\text{hp},\pm}^{(3)}), \quad (61)$$

the last equality in Eq. (61) follows from Eq. (26).

In the 4-loop order, the function $\tilde{T}^{(4)}(a)$ is real only inside the finite interval $(a_1, 0)$ of the negative semi-axis, where a_1 is the root of (13) ($a_1 \approx -0.796$ for $n_f = 3$). The function has a logarithmic branch point at $a = a_1$. The corresponding branch cut may be chosen along the infinite interval $(-\infty, a_1)$. To continue $\tilde{T}^{(4)}(a)$ in the complex a plane, we use formula (55). The limiting values of this analytic function from above and below the left-hand cut are given by

$$\tilde{T}_{\pm}^{(4)}(a) = 1/a - b_1 \ln(|b_1 - 1/|a||) + \text{p.v.} \int_0^a g^{(4)}(s) ds \pm i\kappa\pi, \quad (62)$$

where κ stands for the residue

$$\kappa = \lim_{a \rightarrow a_1} (a - a_1)g^{(4)}(a) = (b_2 + b_3a_1)\{b_3(1 + b_1a_1)(a_1 - a_2)(a_1 - a_3)\}^{-1},$$

and $a_i, i=1..3$, denotes the roots of (13). Formula (54) enables us to define the analytical continuation of the function $\theta = F^{-1(4)}(a)$ in the cut complex a plane. In particular, we need to calculate the boundary values of $F^{-1(4)}(a)$ as $\text{Im}(a) \rightarrow 0^{\pm}$ along the left-hand cut $\{a : -\infty < a < a_1\}$. It is easy to convince that the required branch of W along the sides of the left-hand cut will be $W_0(z)$, provided that $|\kappa/b_1| < 1$. This condition holds only for $0 \leq n_f \leq 5$ (for example, $\kappa/b_1 \approx 0.690$ at $n_f = 3$). Therefore, for $0 \leq n_f \leq 5$, formula (54) is valid also along the sides of the cut. But, for $6 \leq n_f \leq 7$, we have $|\kappa/b_1| > 1$. Then one may check that the relevant branches on the opposite sides of the cut should be $W_{\pm 1}$. We may now calculate the limit of $F^{-1(4)}(a)$ as a approaches infinity going along the upper or lower side of the cut. So we determine the singularities of $F^{(4)}(\theta)$. We use Eq. (54) with Eq. (62) if $0 \leq n_f \leq 5$. However, for $6 \leq n_f \leq 7$, the branch W_0 in Eq. (54) should be replaced by $W_{\pm 1}$. Then we find the singular points

$$\theta_{s,2\pm}^{(4)} = \lim_{a \rightarrow -\infty} F^{-1(4)}(a \pm i0) = \begin{cases} -b_1^{-1}(1 + W_0(\tilde{\zeta}_{\pm}^{(4)}(-\infty)))^{-1} & \text{if } 0 \leq n_f \leq 5 \\ -b_1^{-1}(1 + W_{\pm 1}(\tilde{\zeta}_{\pm}^{(4)}(-\infty)))^{-1} & \text{if } 6 \leq n_f \leq 7 \end{cases} \quad (63)$$

Table 7. Positions of the singularities in the θ -plane at 4-loops. n_1 and n_2 denote the labels of the branches of the W function used to calculate the singularities $\theta_{s,1}$ and $\theta_{s,2\pm}$ respectively. $\tilde{\rho}$ is the radius of convergence of the series (42).

n_f	θ_0	$\theta_{s,1}$	$ \theta_{s,1} $	n_1	$\theta_{s,2\pm}$	$ \theta_{s,2\pm} $	n_2	$\tilde{\rho}$
0	-1.186	0.485	-	-1	$-0.545 \mp 0.334i$	0.639	0	0.485
1	-1.195	0.488	-	-1	$-0.544 \mp 0.341i$	0.642	0	0.488
2	-1.219	0.497	-	-1	$-0.546 \mp 0.354i$	0.650	0	0.497
3	-1.266	0.516	-	-1	$-0.550 \mp 0.380i$	0.668	0	0.516
4	-1.353	0.554	-	-1	$-0.552 \mp 0.429i$	0.699	0	0.554
5	-1.520	0.641	-	-1	$-0.533 \mp 0.526i$	0.748	0	0.641
6	-1.885	0.934	-	-1	$-0.394 \pm 0.672i$	0.779	± 1	0.779
7	-3.008	$-0.887 \mp 1.531i$	1.769	∓ 1	$-0.105 \pm 0.614i$	0.623	± 1	0.623

Table 8. Numerical examination of the series (42) to 3-th and 4-th orders at $n_f = 3$.

n	$\tilde{\rho}_n^{(3)}$	$\tilde{\rho}_n^{(4)}$	n	$\tilde{\rho}_n^{(3)}$	$\tilde{\rho}_n^{(4)}$
10	1.04	0.737	80	0.692	0.550
20	0.807	0.632	90	0.688	0.547
30	0.752	0.597	100	0.685	0.544
40	0.727	0.579	110	0.682	0.542
50	0.713	0.568	120	0.680	0.540
60	0.703	0.560	130	0.678	0.538
70	0.697	0.554	140	0.677	0.537

where $\tilde{\zeta}_{\pm}^{(4)}(-\infty) = (eb_1)^{-1} \exp(-\tilde{T}_{\pm}^{(4)}(-\infty)/b_1)$, and by Eqs. (62) and (26)

$$\tilde{T}_{\pm}^{(4)}(-\infty) = \lim_{a \rightarrow -\infty} \tilde{T}^{(4)}(a \pm i0) = \Re(t_{\text{hfp}\pm}) \pm i\pi\kappa, \quad (64)$$

here the subscript “ \pm ” shows that the limits were evaluated keeping the upper (lower) side of the cut. Evidently, $\theta_{s,2-}^{(4)} = \bar{\theta}_{s,2+}^{(4)}$.

In Tables 6 and 7, we tabulate the singularities $\theta_0(n_f) = -b_1^{-1}$, $\theta_{s,1}^{(k)}(n_f)$ and $\theta_{s,2}^{(k)}(n_f)$ at the 3- and 4-loop orders respectively. In the 3-th order, we see that the singular points $\theta_{s,2}^{(3)}$ are closer to the origin than the points θ_0 or $\theta_{s,1}^{(3)}$, so that the radius of convergence of the series (42) is equal to $|\theta_{s,2}^{(3)}|$. On the contrary, in the 4th order, we find that $\tilde{\rho}^{(4)} = |\theta_{s,1}^{(4)}|$ if $0 \leq n_f \leq 5$, and $\tilde{\rho}^{(4)} = |\theta_{s,2}^{(4)}|$ if $6 \leq n_f \leq 7$. We recall that the radius of convergence of the original series (3) is determined by $\rho^{(k)} = \tilde{\rho}^{(k)}/\beta_0$ ($\rho^{(3)} = 0.965$ and $\rho^{(4)} = 0.720$ for $n_f = 3$).

Looking at the numbers in Tables 6 and 7 one sees that the convergence radii in the range $0 \leq n_f \leq 6$ increases as n_f increases. But, for fixed values of n_f , they decrease as the order of perturbation theory increases. In order to examine the obtained formulas, we calculate numerically the coefficients of the series (42) \tilde{c}_n for large values of n . In Table 8, we study the behaviour of the quantity $\tilde{\rho}_n^{(k)} = (|\tilde{c}_n^{(k)}|)^{-1/n}$ in the 3- and 4-loop orders at $n_f = 3$. It is seen from the table that our predictions are in good agreement with the expected limiting relation $\tilde{\rho}_n^{(k)} \rightarrow \tilde{\rho}^{(k)}$ as $n \rightarrow \infty$. The theoretical predictions are $\tilde{\rho}^{(3)} = 0.653$ and $\tilde{\rho}^{(4)} = 0.516$ for $n_f = 3$ (see Tables 6 and 7).

Table 9. The location of the branch points $a_{1,2}$, a_b and $a_{b\pm}$ of $\theta = F^{-1(3)}(a)$ for $n_f = \{6 - 16\}$.

n_f	a_1	a_2	a_b	$a_{b\pm}$
6	-1.489	7.089	2.418	$-2.258 \pm 0.296i$
7	-0.877	1.238	0.813	$-0.846 \pm 0.101i$
8	-0.651	0.660	0.541	$-0.552 \pm 0.006i$
9	-0.509	0.409	-0.360	$0.439 \pm 0.036i$
10	-0.403	0.264	-0.253	$0.266 \pm 0.034i$
11	-0.318	0.169	-0.177	$0.159 \pm 0.027i$
12	-0.245	0.104	-0.121	$0.089 \pm 0.018i$
13	-0.182	0.059	-0.078	$0.043 \pm 0.011i$
14	-0.125	0.028	-0.044	$0.015 \pm 0.006i$
15	-0.072	0.010	-0.020	$0.002 \pm 0.002i$
16	-0.023	0.001	-0.004	$-0.0013 \pm 0.0002i$

Next consider the theoretical cases with large n_f values where the β -function has non-trivial real zeros. This takes place in the 3-loop case for $n_f = \{6 - 16\}$. From now on we shall confine ourselves to the 3-loop case. There are now two different cases which should be considered separately. For $n_f = \{6 - 8\}$ ($b_1 > 0$ and $b_2 < 0$) the equation $\zeta^{(3)}(a) = -e^{-1}$ has one real positive root a_b ($0 < a_b < a_2$) and a pair of complex conjugate roots $a_{b\pm}$ with $\Re(a_{b\pm}) < 0$ (see Table 9). On the real interval $a_1 < a < a_b$, the real analytic solution to (47) is

$$\theta = \begin{cases} -b_1^{-1}(1 + W_{-1}(z))^{-1} & \text{if } 0 < a < a_b \\ -b_1^{-1}(1 + W_0(z))^{-1} & \text{if } a_1 < a < 0, \end{cases} \quad (65)$$

where $z = \zeta^{(3)}(a)$ (see Eq. (49)). To determine uniquely the analytical continuation of the right-hand side of Eq. (65), we make branch cuts on the a -plane. There are the branch points at $a_{1,2}$, the roots of (13), and at a_b and $a_{b\pm}$, the roots of $\zeta^{(3)}(a) = -e^{-1}$. They are listed in Table 9 as a function of n_f . We make branch cuts along the infinite intervals of the real axis $\{a : -\infty < a < a_1\}$ and $\{a : a_b < a < \infty\}$. There is a double branch cut along the interval $\{a : a_2 < a < \infty\}$. We also make branch cuts along the straight lines joining the points $a_{b\pm}$ with the point a_1 . Now we may continue analytically the function (65) and determine its boundary values along the sides of the right hand cut using the rules of counter-clockwise continuity (58). Choosing the ways along the sides of this cut, we take the limit $a \rightarrow \infty$. Thus we find a pair of complex conjugate singular points

$$\theta_{s,1\pm} = \lim_{a \rightarrow \infty} F^{-1}(a \pm i0) = -b_1^{-1}(1 + W_{\pm n}(z_{\pm}))^{-1}, \quad (66)$$

where $z_{\pm} = \lim_{a \rightarrow \infty} \zeta^{(3)}(a \pm i0)$,

$$z_{\pm} = (eb_1)^{-1} \exp(M_1 \ln(|a_1|)/b_1 - M_2 \ln(a_2)/b_1) \exp(\mp i\pi M_1/b_1),$$

with $M_{1,2} = (a_1 - a_2)^{-1}(1 + b_1 a_{1,2})^{-1}$. It is obvious from Cauchy's theorem that if we calculate the limits choosing the directions along the left-hand cut, we shall reproduce the same values, i.e. $\theta_{s,2\pm} = \theta_{s,1\pm}$. Comparing the modulus of the numbers $\theta_0 = -b_1^{-1}$

Table 10. The locations of the singularities of $a = F(\theta)$ and the convergence radii of the series (42) at 3-loops in the theoretical cases when $n_f = \{6 - 16\}$.

n_f	$W_{\pm n}$	θ_0	$ \theta_{s,1\pm} $	$\tilde{\rho}$
6	$W_{\pm 1}$	1.885	2.114	1.885
7	$W_{\pm 1}$	3.008	0.664	0.664
8	$W_{\pm 19}$	48.17	0.417	0.417
9	$W_{\mp 1}$	2.08	0.291	0.291
10	$W_{\mp 1}$	0.761	0.208	0.208
11	$W_{\mp 1}$	0.360	0.148	0.148
12	$W_{\mp 1}$	0.180	0.102	0.102
13	$W_{\mp 1}$	0.087	0.067	0.067
14	$W_{\mp 1}$	0.037	0.039	0.037
15	$W_{\mp 1}$	0.011	0.018	0.011
16	$W_{\mp 1}$	0.001	0.003	0.001

and $\theta_{s,1\pm}$ (see Table 10), we determine the radii of convergence of the series (42) for $n_f = \{6 - 8\}$. In this Table, we also indicate the required branch of the W function which is used in formula (66).

Next consider the cases with $n_f = \{9 - 16\}$ ($b_1 < 0, b_2 < 0$). Then the equation $\zeta^{(3)}(a) = -e^{-1}$ has a real negative root a_b ($a_1 < a_b < 0$) and a pair of complex conjugate roots $a_{b\pm}$ (see Table 9). The solution to (47) which takes real values inside the real interval $a_b < a < a_2$ is then given by

$$\theta = \begin{cases} -b_1^{-1}(1 + W_0(z))^{-1} & \text{if } 0 < a < a_2 \\ -b_1^{-1}(1 + W_{-1}(z))^{-1} & \text{if } a_b < a < 0, \end{cases} \quad (67)$$

where $z = \zeta^{(3)}(a) = (e|b_1|)^{-1} \exp(T(a)/|b_1|)$. Now we choose the cuts along the real axis $\{a : -\infty < a < a_1\}$, $\{a : -\infty < a < a_b\}$ and $\{a : a_2 < a < \infty\}$. We also make cuts along the straight lines joining the branch points $a_{b\pm}$ with a_2 . By means of the same procedure that was used in the previous case we calculate the locations of the singularities $\theta_{s,1\pm} = \theta_{s,2\pm}$. They are determined by the same formula (66). The relevant branches of W function are listed in Table 10. In this Table, we tabulated the magnitudes of θ_0 , $|\theta_{s,1\pm}| = |\theta_{s,2\pm}|$ and $\tilde{\rho}$, the convergence radius of the series (42), for $n_f = \{6 - 16\}$.

5. The Momentum Scale Associated With the Convergence Radius of the Series

The convergence region of the series (42) in the real momentum squared space may be easily determined, since the mapping $Q^2 \rightarrow \theta = a^{(2)}(Q^2)$ for real positive $Q^2 > Q_L^2 \geq 0$ is monotonic (Q_L^2 being the real Landau singularity of the 2-loop coupling which presents if $0 \leq n_f \leq 8.05$). First, we consider the series for large (mainly unphysical) n_f values. Note that the quantity $\theta_0 = -b_1^{-1}$ in the Banks-Zaks domain ($n_f > 8.05$) is the infrared fixed point of the 2-loop coupling $\theta = a^{(2)}(u)$, so that $0 < \theta < |b_1|^{-1}$ for all $Q^2 \in (0, \infty)$. From the Table 10, we see that $\tilde{\rho} = \theta_0$ inside the interval $n_f = \{14 - 16\}$. This

Table 11. The ratios $\sqrt{u_{\min}^{(k)}} = Q_{\min}^{(k)}/\Lambda$ and $\sqrt{u_{\text{rhp}}^{(k)}} = Q_{\text{rhp}}^{(k)}/\Lambda$ in the $\overline{\text{MS}}$ scheme to the 3- and 4-loop orders for $n_f = \{0 - 6\}$.

n_f	$\sqrt{u_{\min}^{(3)}}$	$\sqrt{u_{\text{rhp}}^{(3)}}$	$\sqrt{u_{\min}^{(4)}}$	$\sqrt{u_{\text{rhp}}^{(4)}}$
0	1.571	1.525	1.790	1.790
1	1.566	1.521	1.788	1.788
2	1.558	1.514	1.784	1.784
3	1.541	1.500	1.773	1.773
4	1.505	1.467	1.745	1.745
5	1.416	1.384	1.678	1.678
6	1.283	–	1.623	1.507

means that the series (42) at 3-loops for $n_f = \{14 - 16\}$ converges in the whole interval $Q^2 \in (0, \infty)$. Let n_f^{**} be the lowest value of n_f for which this equality holds ($n_f^{**} = 14$ in the $\overline{\text{MS}}$ scheme). For $n_f < n_f^{**}$, the series (42) converges in the more restricted domain $Q_{\min}^2 < Q^2 < \infty$ ($Q_{\min}^2 > 0$). The value of Q_{\min}^2 may be determined from the equation

$$\theta = a^{(2)}(u) = -b_1^{-1}(1 + W_n(z_Q))^{-1} = \tilde{\rho} \quad (68)$$

where $z_Q = -(eb_1)^{-1}u^{-1/b_1}$ and $u = Q^2/\Lambda^2$ (see Eq. (2)). Solving (68), we obtain

$$u_{\min} = Q_{\min}^2/\Lambda^2 = (b_1 + \tilde{\rho}^{-1})^{-b_1} \exp(\tilde{\rho}^{-1}).$$

The results for the dimensionless quantity $\sqrt{u_{\min}} = Q_{\min}/\Lambda$ ($Q_{\min} = \sqrt{Q_{\min}^2}$) to the 3- and 4-loop orders, for $n_f = \{0 - 6\}$, are tabulated in Table 11. We compare $\sqrt{u_{\min}}$ with the ratio $\sqrt{u_{\text{rhp}}} = Q_{\text{rhp}}/\Lambda$, where $Q_{\text{rhp}} = \sqrt{Q_{\text{rhp}}^2}$, and Q_{rhp}^2 is the real space-like Landau singularity of the coupling. It is seen from the Table that in general the quantity Q_{\min}^2 can not be identified with the real Landau singularity Q_{rhp}^2 . The equality $Q_{\min}^2 = Q_{\text{rhp}}^2$ occurs only in the cases where the convergence radius $\tilde{\rho}$ is determined via the real (space-like) Landau singularity. This happens, for example, in the $\overline{\text{MS}}$ scheme in the 4-loop case for $n_f = \{0 - 5\}$. However, in the case where $\tilde{\rho}$ is determined via the complex Landau singularities, $Q_{\text{lh}\pm}^2$, the relation between Q_{\min}^2 and $Q_{\text{lh}\pm}^2$ is more complicated. Then we observe the inequality $Q_{\min}^2 > Q_{\text{rhp}}^2$. Such a situation occurs, for instance, in the $\overline{\text{MS}}$ scheme in the 3-loop case for $n_f = \{0 - 5\}$.

It is reasonable to compare Q_{\min} with the infrared boundary of QCD, the momentum scale μ_c that separates the perturbative and nonperturbative regimes of the theory in the confining phase. Several estimates for this quantity was suggested using different nonperturbative methods. In recent work [20] an useful nonperturbative approximation for the QCD β -function has been constructed. The model gives a number consistent results for various nonperturbative quantities. In particular, it was obtained that $(\mu_c/\Lambda_{\text{QCD}})_{3\text{-loop}} \approx 3.204$ and $(\mu_c/\Lambda_{\text{QCD}})_{4\text{-loop}} \approx 3.526$ with the perturbative $\overline{\text{MS}}$ scheme component of the total β -function in the 3-th and 4-th orders. Other approach to determine the infrared boundary is to use arguments based on dynamical chiral symmetry breaking in QCD. There are the results obtained within the nonperturbative framework of Schwinger-Dyson equations [42, 43]. It was found in ref. [42] that the

critical value of the coupling needed to generate the chiral condensate is $\alpha_c = \pi/4$ (for $N_c = 3$ QCD). It is reasonable to identify the corresponding scale with the infrared boundary [49]. To obtain approximations to μ_c , we may use the perturbative expressions for the coupling in the $\overline{\text{MS}}$ scheme. With this simplifying assumption, the equation $\alpha_s^{(k)}(\mu_c^2) = \pi/4$ in the 3- and 4-loop orders, for $n_f = 3$, yields the estimates

$$(\mu_c/\Lambda_{\overline{\text{MS}}})_{3\text{-loop}} = 1.972 \quad \text{and} \quad (\mu_c/\Lambda_{\overline{\text{MS}}})_{4\text{-loop}} = 2.115.$$

The two different estimates considered above are consistent with the inequality $Q_m^2 < \mu_c^2$. Thus it seems reasonable to believe that the series expansion (42) in the $\overline{\text{MS}}$ scheme may be safely used in the whole perturbative region $\mu_c^2 < Q^2 < \infty$.

6. Application to Analytic Perturbation Theory

In the Analytic Perturbation Theory (APT) approach of Shirkov and Solovtsov, Euclidean and Minkowskian QCD observables (which depend on the single scale) are represented by asymptotic expansions over non-power sets of specific functions $\{\mathcal{A}_n^{(k)}(u)\}_{n=1}^{\infty}$ and $\{\mathfrak{A}_n^{(k)}(\bar{s})\}_{n=1}^{\infty}$ respectively (see refs. [11, 12]), here $u = Q^2/\Lambda^2$ and $\bar{s} = s/\Lambda^2$. These sets are constructed via the integral representations in the following way

$$\mathcal{A}_n^{(k)}(u) = \frac{1}{\pi} \int_0^\infty \frac{\varrho_n^{(k)}(\varsigma) d\varsigma}{\varsigma + u}, \quad \mathfrak{A}_n^{(k)}(\bar{s}) = \frac{1}{\pi} \int_{\bar{s}}^\infty \frac{\varrho_n^{(k)}(\varsigma) d\varsigma}{\varsigma}, \quad (69)$$

where the spectral densities to the k -th order are determined from powers of the running coupling: $\varrho_n^{(k)}(\varsigma) = -\Im(a^{(k)n}(-\varsigma + i0))$. In APT the power series (42) give rise to the following series of functions

$$\mathcal{A}_m^{(k)}(u) = \sum_{n=m}^{\infty} \mathcal{C}_{m,n}^{(k)} \mathcal{A}_n^{(2)}(u) \quad m = 1, 2, \dots \quad (70)$$

$$\mathfrak{A}_m^{(k)}(\bar{s}) = \sum_{n=m}^{\infty} \mathcal{C}_{m,n}^{(k)} \mathfrak{A}_n^{(2)}(\bar{s}) \quad m = 1, 2, \dots \quad (71)$$

$$\varrho_m^{(k)}(\varsigma) = \sum_{n=m}^{\infty} \mathcal{C}_{m,n}^{(k)} \varrho_n^{(2)}(\varsigma) \quad m = 1, 2, \dots, \quad (72)$$

where $\mathcal{C}_{m,m}^{(k)} = 1$. The sets of coefficients $\{\mathcal{C}_{m,n}^{(k)}\}_{n=m}^{\infty}$, $m = 1, 2, \dots$, are constructed from the set of coefficients of the original series, $\{\tilde{\mathcal{C}}_n^{(k)}\}_{n=1}^{\infty}$, according to the rules for products of power series: $\mathcal{C}_{1,n}^{(k)} = \tilde{\mathcal{C}}_n^{(k)}$, $\mathcal{C}_{2,n}^{(k)} = \sum_{j=1}^{n-1} \tilde{\mathcal{C}}_{n-j}^{(k)} \tilde{\mathcal{C}}_j^{(k)}$ etc. The spectral densities at the 2-loop order can be expressed analytically in closed form [32, 50]

$$\varrho_n^{(2)}(\varsigma) = b_1^{-n} \Im(1 + W_{-1}(z_\varsigma))^{-n} \quad \text{with} \quad z_\varsigma = (eb_1)^{-1} \varsigma^{-1/b_1} \exp(-i\pi(1/b_1 - 1)). \quad (73)$$

Now we are going to prove that the series of functions (70), (71) and (72) are uniformly convergent over whole ranges of the corresponding variables: $0 < u < \infty$, $0 < \bar{s} < \infty$ and $0 < \varsigma < \infty$. Suppose that the series (72) is uniformly convergent. Then the series (70) and (71) will also be uniformly convergent. To see this, let us insert the series (72) into integral representations given in (69) and integrate term-by-term. This yields the

Table 12. The quantity θ_{\max} versus the convergence radii $\tilde{\rho}^{(k)}$.

n_f	0	1	2	3	4	5	6
θ_{max}	0.237	0.237	0.238	0.240	0.243	0.249	0.259
$\tilde{\rho}^{(3)}$	0.594	0.601	0.618	0.653	0.731	0.956	1.885
$\tilde{\rho}^{(4)}$	0.485	0.488	0.497	0.516	0.554	0.641	0.779

series (70) and (71), which must be uniformly convergent, as results of term-by-term integration of the uniformly convergent series. Evidently, the factors $1/(\zeta + u)$ and $1/\zeta$ inside the integrals will not destroy this statement.

Let us now write $W_{-1}(z_c) = \mathcal{W} = \mathcal{X} + i\mathcal{Y}$, $(1 + \mathcal{W})^{-1} = \mathcal{R} \exp(i\Psi)$, where $\mathcal{R} = ((\mathcal{X} + 1)^2 + \mathcal{Y}^2)^{-1/2}$ and $\Psi = \arcsin(-\mathcal{Y}\mathcal{R})$ (for the branch W_{-1} , we have $-3\pi < \mathcal{Y} < 0$). According to this, we may rewrite the 2-loop spectral densities (73) as

$$\varrho_n^{(2)}(\zeta) = (\mathcal{R}/b_1)^n \sin(n\Psi), \quad n = 1, 2, \dots \quad (74)$$

It is seen from Eq. (74) that the modulus of the spectral densities are bounded above

$$|\varrho_n^{(2)}(\zeta)| < (\theta_{\max})^n, \quad (75)$$

where $\theta_{\max} = \mathcal{R}_{\max}/b_1$ and \mathcal{R}_{\max} is the maximal value of \mathcal{R} in the range $0 < \zeta < \infty$. We find useful to use the ‘‘Maple 7’’ [47] for determining \mathcal{R}_{\max} numerically. In Table 12, we listed numerical values of θ_{\max} in the phenomenologically interesting case $n_f = \{0 - 6\}$. Note that all the power series $\sum_{n=m}^{\infty} \mathcal{C}_{m,n}^{(k)} \theta^n$, $m = 1, 2, \dots$, have the same radius of convergence, $\tilde{\rho}^{(k)}$, as the original series (42). This follows from the definition

$$\sum_{n=m}^{\infty} \mathcal{C}_{m,n}^{(k)} \theta^n = \left(\sum_{l=1}^{\infty} \tilde{c}_l^{(k)} \theta^l \right)^m. \quad (76)$$

Consider now the set of numerical series of positive terms

$$\sum_{n=m}^{\infty} |\mathcal{C}_{m,n}^{(k)}| \theta_{max}^n \quad m = 1, 2, \dots, \quad (77)$$

looking at the numbers in Table 12, we see that θ_{\max} is inside the convergence disk of the series (76), $0 < \theta_{\max} < \tilde{\rho}^{(k)}$. Hence all the numerical series (77) are convergent. Combining this fact with the bounding conditions (75), we find that the series of functions $\sum_{n=m}^{\infty} |\mathcal{C}_{m,n}^{(k)}| \varrho_n^{(2)}(\zeta)$, $m = 1, 2, \dots$, are uniformly convergent by the comparison test due to Weierstrass. Then all the series (72) are uniformly convergent. Hence by the arguments given above, the series of functions (70) and (71) are also uniformly convergent.

The series (70) and (71) enable us to calculate the infrared limits of the APT expansion functions. Thus we may reproduce remarkable results of Shirkov and Solovtsov [7, 10] in a mathematically rigorous way ¶. It is seen from the definition (69) that $\lim_{u \rightarrow 0^+} \mathcal{A}_n^{(k)}(u) = \lim_{\bar{s} \rightarrow 0^+} \mathfrak{A}_n^{(k)}(\bar{s})$. Therefore, we shall consider only the Minkowskian set of functions. In the 2-loop order, one may calculate the infrared limits

¶ An alternative derivation of these results in the context of the asymptotic solutions to the RG equation was recently given in ref. [19].

of the expansion functions using the explicit formulas obtained in ref. [50]. The first two Minkowskian functions are given by

$$\mathfrak{A}_1^{(2)}(\bar{s}) = 1 - \pi^{-1} \Im \ln W_1(z_s), \quad \mathfrak{A}_2^{(2)}(\bar{s}) = \pi^{-1} b_1^{-1} \Im \ln \{W_1(z_s)/(1 + W_1(z_s))\}, \quad (78)$$

where $z_s = (eb_1)^{-1} \bar{s}^{-1/b_1} \exp(i\pi(1/b_1 - 1))$. The functions with higher values of index are determined by the recurrence relation (see ref. [50])

$$\mathfrak{A}_{n+2}^{(2)}(\bar{s}) = -b_1^{-1} \left(\mathfrak{A}_{n+1}^{(2)}(\bar{s}) + \frac{1}{n} \frac{d}{d \ln \bar{s}} \mathfrak{A}_n^{(2)}(\bar{s}) \right). \quad (79)$$

The asymptotics of $W_1(z_s)$ as $|z_s| \rightarrow \infty$ may be determined using Eq. (27) with $L_1 = \ln z_s + i2\pi$ [4]. Combining (78) and (79) and taking the limit $\bar{s} \rightarrow 0^+$, we find

$$\mathfrak{A}_n^{(2)}(\bar{s}) \approx \delta_{n,1} + (1 + b_1) \ln^{-n} \bar{s} + O(\ln^{-n-1} \bar{s}) \rightarrow \delta_{n,1}, \quad (80)$$

hence $\lim_{u \rightarrow 0^+} \mathcal{A}_n^{(2)}(u) = \lim_{\bar{s} \rightarrow 0^+} \mathfrak{A}_n^{(2)}(\bar{s}) = \delta_{n,1}$. These relations may be extended to higher orders by means of the expansions (70) and (71). Thus we can write

$$\lim_{u \rightarrow 0^+} \mathcal{A}_m^{(k)}(u) = \sum_{n=m}^{\infty} \mathcal{C}_{m,n}^{(k)} \lim_{u \rightarrow 0^+} \mathcal{A}_n^{(2)}(u) = \mathcal{C}_{m,1}^{(k)} \equiv \delta_{m,1}, \quad (81)$$

the calculation of the limit of the sum of the series term-by-term, as $u \rightarrow 0$, is justified by the uniform convergence of the series. It should be stressed that these results (in particular, finiteness of $\mathcal{A}_1^{(k)}(0)$ originally obtained in [7]) are direct consequences of the asymptotic freedom (AF) of the theory. This interesting relationship has been recently elucidated by the author of ref. [19] using a different technique. In this connection, we remark that the recurrence formula (79) follows directly from the AF, as it was shown in refs. [50, 32]. The universality of $\mathcal{A}_1^{(k)}(0)$ and $\mathfrak{A}_1^{(k)}(0)$ (the scheme independence and invariance with respect to higher-loop corrections) is evident.

7. Conclusion

The main objective of this investigation was to study convergence properties of the new expansion (3). In section 2 we have systematically discussed the analyticity structure of the modified coupling $a(Q^2/\Lambda^2)$ at 3- and 4-loops in the complex $u = Q^2/\Lambda^2$ plane for all n_f values in the range $0 \leq n_f \leq 16$. For higher values of n_f , when the β -function has only real zeros, we have reproduced the part of results of refs. [16, 17] using a different technique. For low values of n_f , when the β -function has complex zeros, we have determined the analytical continuation of the function $t = T(a)$ choosing the cuts properly in the complex coupling plane. With this choice, we have found that the running coupling has a pair of complex conjugate singular points in the first Riemann sheet of the Q^2 plane besides the real singularity on the positive semi-axis. In many cases, just these complex singularities determine the radius of convergence of the series (3) (e.g. $0 \leq n_f \leq 5$ at 3 loops).

In section 3 we have proved that in the $\overline{\text{MS}}$ -like schemes the power series (3) has a finite radius of convergence to all orders in perturbation theory for all $n_f = 0 - 16$. Therefore, the series inside its circle of convergence represents the exact solution to

the RG equation (A.1). In the proof, we have used methods of analytical theory of differential equations.

In section 4 we have determined the analytical structure of the modified coupling in higher orders as a function of the 2-loop order coupling θ ($\theta = a^{(2)}(Q^2/\Lambda^2)$). We have considered the 3- and 4-loop cases for $0 \leq n_f \leq 16$ and $0 \leq n_f \leq 7$ respectively. We have found helpful Eq. (48), the implicit solution for the higher order coupling determined via the Lambert-W function. By means of this formula, we have determined the analytical continuation of the inverse function $\theta = F^{-1}(a)$ in the complex a plane. This enabled us to find the locations of the singularities of the coupling $a = F(\theta)$ in the θ -plane (see Tables 6 and 7). The correspondence between the singularities of the coupling in the Q^2 and θ planes has been established. Comparing various singularities of the coupling in the θ -plane, we have determined the radii of convergence of the series (42) $\tilde{\rho}^{(k)}$. From a practical viewpoint, the radii of convergence of the original series (3), $\rho^{(k)} = \tilde{\rho}^{(k)}/\beta_0$, is found to be sufficiently large. For example, $\rho^{(3)} = 0.965$ and $\rho^{(4)} = 0.720$ at $n_f = 3$. The obtained predictions for the convergence radius have been examined by the independent numerical calculation. One further important property of the series is high convergence rate. In previous papers [32, 36], we observed that in the 3- and 4-loop orders partial sums of these series with the first few terms give very good approximations to the coupling even in the infrared region. This was confirmed in conventional perturbation theory as well as in APT.

In section 5 we have determined the convergence region of the series (42) in the momentum squared space. For sufficiently large n_f values ($n_f \geq 14$ in the $\overline{\text{MS}}$ scheme), we have found that the series converges in the whole physical range $0 < Q^2 < \infty$. For lower n_f values, we have evaluated the lower boundary of the convergence region Q_{min}^2 . We have compared this scale with the estimations of the infrared boundary of QCD, μ_c , obtained within two different non-perturbative approaches and found that $Q_{\text{min}}^2 < \mu_c^2$. This is in agreement with the possibility that the series (3) in the $\overline{\text{MS}}$ scheme may be used safely in the whole perturbative region $\mu_c^2 < Q^2 < \infty$.

In section 6 we have studied the convergence properties of the non-power series constructed from the series (42) according to the rules of the QCD Analytic Perturbation Theory of Shirkov and Solovstov both in the space- and time-like regions. We have shown that the Euclidean and Minkowskian variants of these non-power series are uniformly convergent over whole domains of the corresponding momentum squared variables. A mathematically rigorous proof of an interesting result of ref. [7], the finiteness and universality of the analytic coupling at zero momentum, has been presented.

The series solution (3) may be useful in high-precision calculations of QCD observables beyond the 2-loop order in low-momentum regime. It clearly provides more accurate results than the standard asymptotic expansion (28) for the coupling (see ref. [36]). This series may be used in different variants of the analytic approach to perturbative QCD suggested in refs. [9, 18, 22, 23]. It may also be applied in the contexts of the ‘‘contour improved’’ perturbation theory of refs. [26-31] and resummation methods proposed in refs. [51] and [52]. Another possible application of the series is to

construct the running coupling with consistent matching conditions at quark thresholds in MS-like renormalization schemes [12, 19, 50, 53].

Acknowledgments

I would like to thank D. V. Shirkov for helpful advises. The author have enjoyed discussions on this subject with A. L. Kataev, A. A. Khelashvili, A. N. Kvinikhidze, S. V. Mikhailov and I. L. Solovtsov. The present work has been partly supported by the Georgian Research and Development Foundation under grant No, GEP2-3329-TB-03.

Appendix

The RG equation to the k -th order reads

$$\frac{d\alpha_s(Q^2)}{d\ln Q^2} = \beta^{(k)}(\alpha_s(Q^2)) = - \sum_{n=0}^{k-1} \beta_n \{\alpha_s(Q^2)\}^{n+2}, \quad (\text{A.1})$$

the running coupling satisfies the normalization condition $\alpha_s(\mu^2) = g^2/(4\pi)$, where μ is the renormalization point and g is the gauge coupling of QCD. In the class of schemes where the β -function is mass independent β_0 and β_1 are universal

$$\beta_0 = (4\pi)^{-1}(11 - 2n_f/3), \quad \beta_1 = (4\pi)^{-2}(102 - 38n_f/3). \quad (\text{A.2})$$

The results for the coefficients β_2 and β_3 in the \overline{MS} scheme can be found in refs. [54] and [55]

$$\beta_2 = (4\pi)^{-3}(2857/2 - 5033n_f/18 + 325n_f^2/54) \quad (\text{A.3})$$

$$\begin{aligned} \beta_3 = (4\pi)^{-4} & \left(\frac{149753}{6} + 3564\zeta_3 - \left(\frac{1078361}{162} + \frac{6508}{27}\zeta_3 \right) n_f \right. \\ & \left. + \left(\frac{50065}{162} + \frac{6472}{81}\zeta_3 \right) n_f^2 + \frac{1093}{729}n_f^3 \right), \end{aligned} \quad (\text{A.4})$$

here ζ is the Riemann zeta-function ($\zeta_3 = 1.202056903\dots$). The values of the first three coefficients $b_{1,2,3}$ ($b_n = \beta_n/\beta_0^{n+1}$) in the \overline{MS} scheme are tabulated in Table A.1.

References

- [1] Gardi, E., Grunberg, G., Karliner, M.: J. High Energy Phys. **07**, 007 (1998)
- [2] Magradze, B. A.: In: Proceedings of the 10th International Seminar ‘‘QUARKS-98’’ Suzdal, Russia, 1998 (Bezrukov F. L., et al.: eds.), vol 1, p. 158, Moscow: Russian Academy of Sciences, Institute for Nuclear Research 1999; Magradze, B. A.: Proc. A. Razmadze Mathematical Institute **118**, 111 (1998)
- [3] Appelquist, T., et al.: Phys. Rev. **D58**, 105017 (1998)
- [4] Corless, R. M., et al.: Advances in Computational Mathematics **V5**, 329 (1996).
- [5] Magradze, B. A.: Int. J. Mod. Phys. **A15**, 2715 (2000)
- [6] Dokshitzer, Yu., Marchesini, G., Webber, B. R.: Nucl. Phys. **B469**, 93 (1996); Dokshitzer Yu., Khoze, V. A., Troyan, S. I.: Phys. Rev. **D53**, 89 (1996)

Table A1. The $\overline{\text{MS}}$ -scheme $\bar{\beta}$ function coefficients $b_{1,2,3}$ for $n_f = 0 - 16$.

n_f	b_1	b_2	b_3	n_f	b_1	b_2	b_3
0	102/121	2857/2662	1.9973	9	-12/25	-1201/250	1.0105
1	804/961	62365/59582	1.9913	10	-222/169	-41351/4394	5.0716
2	690/841	48241/48778	1.9449	11	-336/121	-49625/2662	21.273
3	64/81	3863/4374	1.8428	12	-50/9	-6361/162	84.088
4	462/625	21943/31250	1.6662	13	-564/49	-64223/686	360.81
5	348/529	9769/24334	1.3969	14	-678/25	-70547/250	2009.6
6	26/49	-65/686	1.0297	15	-88	-2823/2	21254
7	120/361	-12629/13718	0.6107	16	-906	-81245/2	2263651
8	6/289	-22853/9826	0.3549				

- [7] Shirkov D. V., Solovtsov, I. L.: Phys. Rev. Lett. **79**, 1209 (1997)
- [8] Shirkov, D. V.: Nucl. Phys. (Proc. suppl.) **B64**, 106 (1998)
- [9] Milton, K. A., Solovtsov, I. L., Solovtsova, O. P.: Phys. Lett. **B415**, 104 (1997)
- [10] Solovtsov, I. L., Shirkov, D. V.: Theor. Math. Phys. **120**, 1220 (1999)
- [11] Shirkov, D. V.: Lett. Math. Phys. **48**, 135 (1999)
- [12] Shirkov, D. V.: Theor. Math. Phys. **127**, 409 (2001); Shirkov, D. V.: Eur. Phys. J. **C22**, 331 (2001)
- [13] Shirkov, D. V.: Theor. Math. Phys. **132**, 1309 (2002)
- [14] Shirkov, D. V.: hep-ph/0510247; Shirkov, D. V., Zayakin, A. V.: hep-ph/0512325
- [15] Grunberg, G.: JHEP **11**, 006 (1998); Grunberg, G.: JHEP **03**, 024 (1999)
- [16] Gardi, E., Grunberg, G.: JHEP **03**, 024 (1999)
- [17] Gardi, E., Karliner, M.: Nucl. Phys. **B529**, (1,2), 383 (1998)
- [18] Alekseev, A. I., Arbuzov, B. A.: Mod. Phys. Lett. **A13**, 1747 (1998); Alekseev, A. I.: 2000 Phys. Rev. **D61**, 114005 (2000); Alekseev, A. I.: J. Phys. **G27**, L117 (2001); Alekseev, A. I.: hep-ph/0503242
- [19] Alekseev, A. I.: Few-Body Systems **32**, 193 (2003)
- [20] Alekseev, A. I., Arbuzov, B. A.: Mod. Phys. Lett. **A20**, 103 (2005)
- [21] Nesterenko, A. V: Int. J. Mod. Phys. **A18**, 5475 (2003); Nesterenko, A. V., Papavassiliou, J.: Phys. Rev. **D71** 016009 (2005)
- [22] Cvetič, G., Valenzuela, C., Schmidt, I.: hep-ph/0508101; Cvetič, G., Valenzuela, C.: hep-ph/0601050
- [23] Bakulev, A. P., Mikhailov, S. V., Stefanis, N. G.: Phys. Rev. **D72**, 074014 (2005); Bakulev, A. P., Karanikas, A. I., Stefanis, N. G.: Phys. Rev. **D72** 074015 (2005); Bakulev, A. P., Stefanis, N. G.: Nucl. Phys. **B721** 50 (2005); Bakulev, A. P., et al.: Phys. Rev. **D70** 033014 (2004)
- [24] Prospero, G. M., Raciti, M., Simolo, C.: hep-ph/0607209
- [25] Krasnikov, N. V., Pivovarov, A. A.: Mod. Phys. Lett. **A11**, 835 (1996)
- [26] Pivovarov, A. A.: Sov. J. Nucl. Phys. **54**, 676 (1991); Pivovarov, A. A.: Z. Phys. **C53**, 461 (1992); hep-ph/0302003; Pivovarov, A. A.: Nuovo Cim. **A105**, 813 (1992); Pivovarov, A. A.: Atom. Nucl. **66**, 724 (2003)
- [27] Groote, S., Körner, J. G., Pivovarov, A. A.: Mod. Phys. Lett. **A13**, 637 (1998)
- [28] Le Diberger, F., Pich, A.: Phys. Lett. **B286** 147 (1992)
- [29] Kataev, A. L., Starshenko, V. V.: Mod. Phys. Lett. **A10**, 235 (1995)
- [30] Raczka, P. A., Szymacha, A.: Z. Phys. **C70**, 125 (1996); Raczka, P. A.: hep-ph/0602085
- [31] Howe, D. M., Maxwell, C. J.: Phys. Lett. **B541**, 129 (2002); Howe, D. M., Maxwell, C. J.: Phys. Rev. **D70**, 014002 (2003)

- [32] Kourashev, D. S., Magradze, B. A.: *Theor. Math. Phys.* **135**, 531 (2003)
- [33] Kourashev, D. S.: hep-ph/9912410
- [34] Maxwell, C. J., Marjalili, A.: *Nucl. Phys.* **B577**, 209 (2000)
- [35] Rodrigo, G. Pich, A., Santamaria, A.: *Phys. Letters* **B424**, 367 (1998)
- [36] Magradze, B. A.: hep-ph/0305020
- [37] Banks, T., Zaks, A.: *Nucl. Phys.* **B196**, 189 (1982)
- [38] Miransky, V. A.: *Phys. Rev.* **D59**, 105003 (1999)
- [39] Oehme, R., Zimmerman, W.: *Phys. Rev* **D21**, 471 (1980); Oehme, R.: *Phys. Rev.* **D42**, 4209 (1990); Nishijima, K.: *Prog. Theor. Phys* **75**, 1221 (1986)
- [40] Bardeen, W. A., et al.: *Phys. Rev.* **D18**, 3998 (1978)
- [41] Stevenson, P. M.: *Phys. Rev.* **D23**, 2916 (1981)
- [42] Fomin, P. I., et al.: *Riv. Nuovo Cimento* **6**, 1 (1983)
- [43] Roberts, C. D., Williams, A. G.: *Prog. Part. Nucl. Phys.* **33**, 477 (1994)
- [44] Bethke, S.: *J. Phys.* **G26**, R27 (2000)
- [45] Ince, E. L.: *Ordinary Differential Equations*. New York: Dover 1956
- [46] Fuks, B. A., Levin, V. I.: *Functions of complex variables and their applications: special topics*. Moscow: State publishing house 1951 (in russian)
- [47] Corless, R. M.: *Essentials Maple 7*. New York: Springer-verlag Inc. 2002
- [48] Hurwitz, A., Courant, R.: *The theory of functions*. Moscow: Nauka 1968 (in russian)
- [49] Chishtie F. A., et all.: *Prog. Theor. Phys.* **104**, 603 (2000)
- [50] Magradze, B. A.: *Comm. of the Joint Institute for Nuclear Research* **E2-2000-222**, 2 (2000)
- [51] Maxwell, C. J.: *Phys. Lett.* **B409**, 450 (1997)
- [52] Cvetič, G.: *Phys. Rev.* **D57**, 3209 (1998)
- [53] Rodrigo, G.: *Phys. Lett.* **B313**, 441 (1993)
- [54] Tarasov, O. V., Vladimirov, A. A., Zharkov, A. Yu.: *Phys. Lett.* **B93**, 429 (1980)
- [55] Van Ritberger T., Vermaseren, J. A. M., Larin, S. A.: *Phys. Lett* **B400**, 379 (1997)